



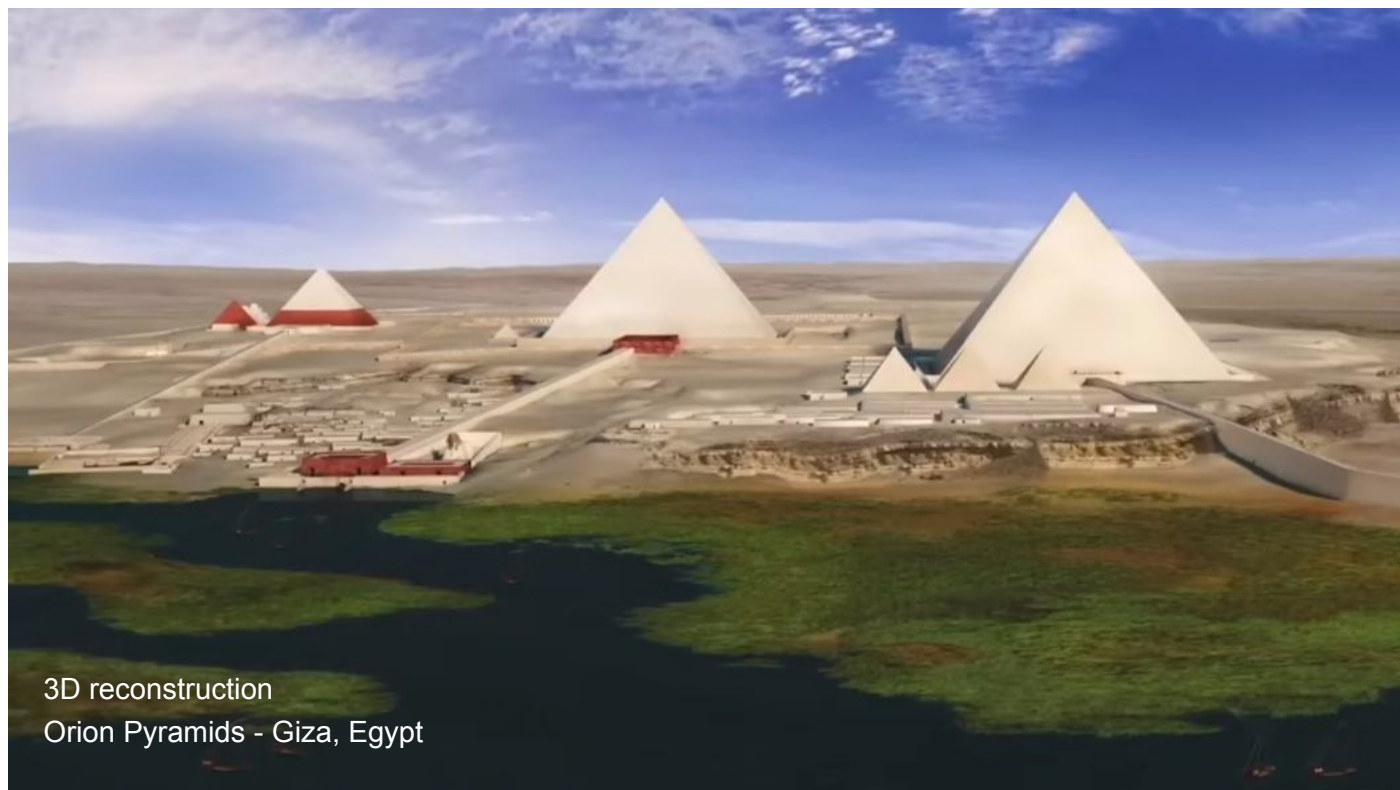
4

The Fire of Life

The Fire of Life

Multidisciplinary investigations have driven many developments in our understanding of the extraordinary technological capabilities of the original builders of the Orion Pyramid Complex of Giza, Egypt. Muon scanning has revealed the hidden presence of large chambers in the Great Pyramid that have yet to be entered in modern times, as well as an alternate entry tunnel hidden behind the large chevron blocks.¹

These new discoveries have been consistently met with resistance from Egyptian officials, who have purposefully stalled the progress of this research to a virtual crawl by repeatedly denying access to investigators. This long-term obfuscation plan has been strategically coordinated within a larger government conspiracy to indefinitely conceal the closely related extraterrestrial UFO reality from the general public.



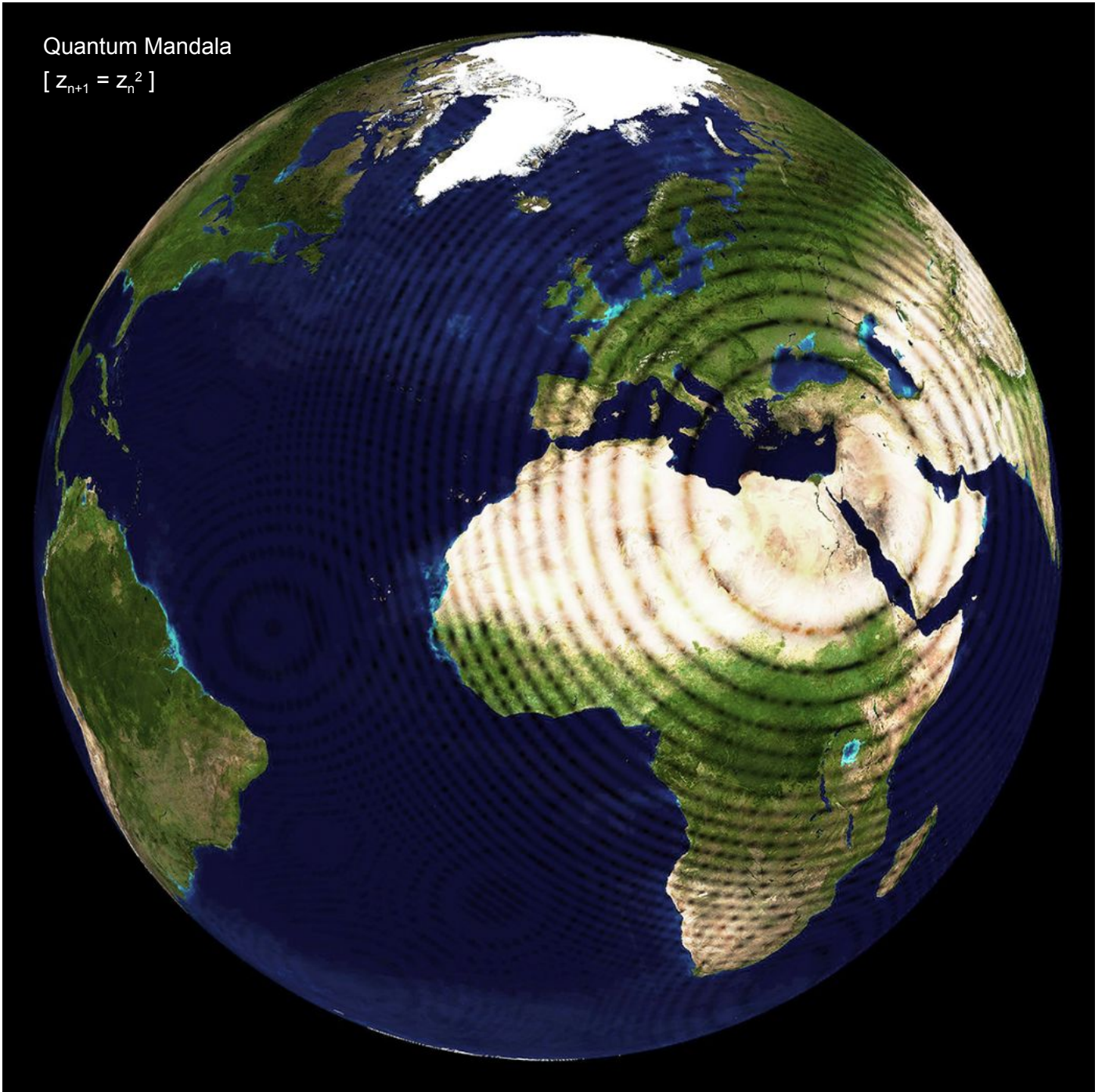
Why are these two cover-ups so closely related? To answer this broader question, we must recognize the world's ancient pyramids as atmospheric resonators that provide EM power for underground cities and advanced aerospace vehicles. While UFO spacecraft have been widely acknowledged as incorporating radioactive metals into their electrogravitic hulls, the general public remains completely unaware of the presence of radioactive metals *incorporated into architectural features of the Orion Pyramids of Giza, Egypt*.

A major set of archeological and quantum physics discoveries await investigation within those unmapped, sealed sections of the Great Pyramid, and all progress in this direction appears to be inextricably linked with a ramped-up UFO disclosure process driven by the US Congressional Oversight Committee. Concurrence of these government disclosure programs implicates an impending release of ET technological information.

It is known that red granite blocks comprising the walls of the pyramids inner chambers and resonator boxes contain radium traces, known as a potent γ -ray emitter. Less well-known is the presence of natural monazite sands filling unmapped corridors within the Great Pyramid, which also contain radioactive components that have been entirely overlooked by all researchers of the monument. Long-lived radionuclides have also been reported in comprehensive chemical analyses of orange-red metal oxide deposit samples obtained from the Giza Plateau near the Central Pyramid, and from within chambers of the Great Pyramid and Red Pyramid.²

Quantum Mandala

$$[z_{n+1} = z_n^2]$$



Two decades of investigation by this author have positively identified hundreds of ancient Atlantean pyramids and megalithic temple sites distributed throughout the globe, comprehensively defining the mandala pattern of infrasound standing wave resonance defined by the function $[z_{n+1} = z_n^2]$ (above). This application of orthogonal standing waves was rediscovered by Nikola Tesla at Colorado Springs in 1898.³

Powerful psychoacoustic effects of biorhythmic synchronization were experienced at every Atlantean temple site within the worldwide network, which included hundreds of subterranean complexes housing advanced technological developments –many of which are still covertly occupied today. Certainly, the governments of all countries with large territories have long been involved in the tracking of advanced aerospace vehicles to and from subterranean bases. This much is revealed by the strategic positioning of missile testing ranges, weaponized Doppler radar sites and top-secret aerospace testing facilities –set up right next to ET bases for targeting spacecraft traffic monitored at each site. Downed spacecraft are hauled out for retro-engineering.

Concealing the covert, black budget UFO surveillance, targeting and crash retrieval programs is far easier to accomplish than hiding similarly advanced technologies incorporated into geopolymer stone landforms at Paleo-Sanskrit pyramid sites distributed throughout the world. Special knowledge concerning the pyramids emerged in the Cassiopaea transmissions of Laura Knight-Jadczyk and her group on November 19, 1994:

Q: (L) What were the physical dimensions of these [Atlantean] crystals and were they cut or naturally grown?

A: Varied. Were synthetic [geopolymer stone constructions]...

Q: (L) How large was the largest from base to apex? A: 5000 feet.

Q: (L) What was the average size? A: 500 feet.

Q: (L) And was the one that was 5,000 feet tall, is that one still in existence? A: Yes.

Q: (L) Where is that one located? A: 380 miles due east of you? [ie. east of Jacksonville, Florida]

Q: (L) Some years ago a pilot reported seeing a pyramid near there in the water...

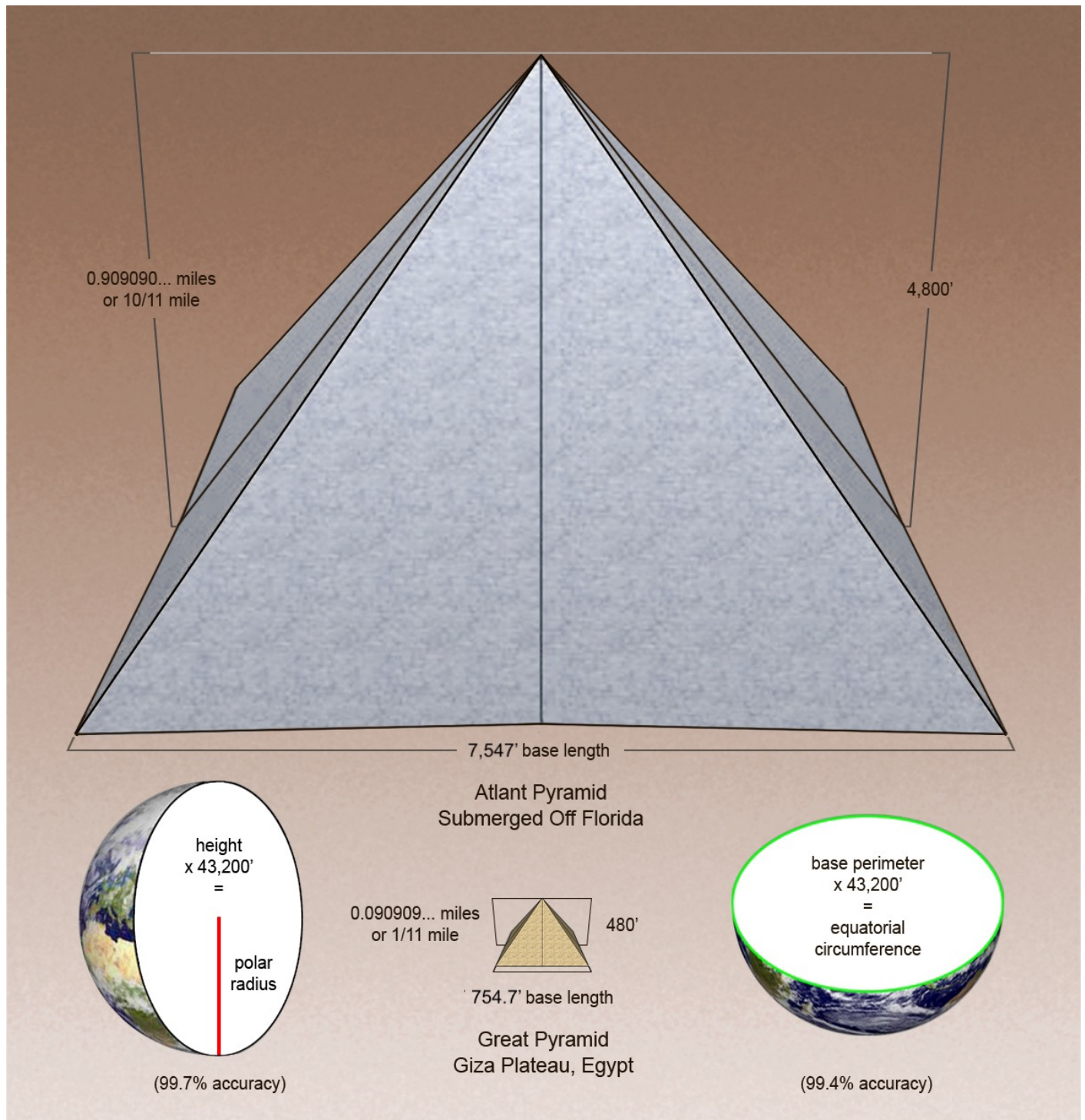
A: That is just the top sticking out of the ocean floor. It is 90 percent buried.



Information imparted by the Cs corroborates detailed teachings published by the Eduard Meier UFO contact group in Switzerland, revealing the Great Pyramid had been designed and geometrically encoded after the majestic Atlant Pyramid, constructed ~133,000 years ago by a Plejaren ET colony established on Earth.

Many features that were specifically encoded into the geopositioning and dimensional proportions of the Great Pyramid of Egypt show parallels to those of the Atlant Pyramid, now submerged in a few thousand feet of water at the edge of the Blake Escarpment off Florida's east coast. The Atlant Pyramid's latitude precisely matches that of the Great Pyramid, at exactly 29.9792458° North latitude, reflecting the speed of light: 29.9792458 m/s. This fact confirms the advanced mathematical and technological prowess of its builders.

This high-precision geoposition clearly references the temples' biophotonic function, confirming minutes and seconds as Atlantean units of time measurement. This fact parallels my previous identification of the mile as an Atlantean unit calibrated to Earth's mean circumference, using Fibonacci #139 ($50.09... \times 10^{-27}$) in percent and Fibonacci #361 ($12,446.66... \times 10^{-71}$) in miles. This highly significant finding was shared in my first book 'Phi', in the context of global distribution calculations provided for major pyramid, temple and megalith sites.

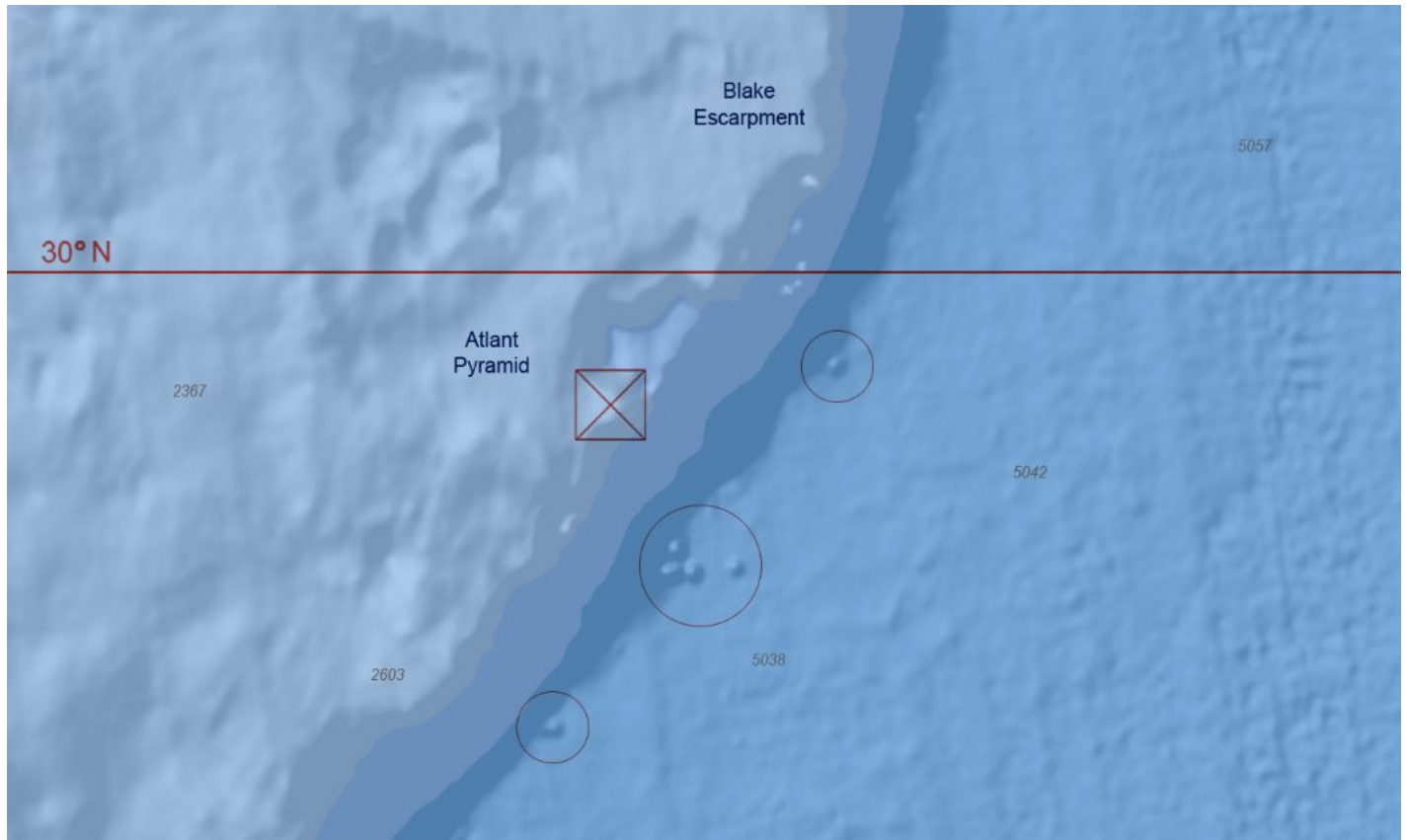


Rounded figures mentioned by the Cassiopaeans suggest the original height of the Atlant Pyramid is 4,800', corresponding to exactly 10 times the size of the Great Pyramid of Giza, standing at 480' (above). Because the submerged Atlant Pyramid and the Great Pyramid are geometrically scaled 10:1, all the high-precision mathematical features encoded in dimensions of the Great Pyramid may also apply to the Atlant Pyramid.

Earth's polar radius and equatorial circumference have also been encoded into the dimensions of the Great Pyramid. The height of Great Pyramid of Giza is $\frac{1}{11}$ of a mile, or 0.090909... miles, whereas the height of the Atlant Pyramid is $\frac{10}{11}$ of a mile, or 0.909090... miles. Thus, the combined heights of both pyramids is exactly 1 mile, or 5,280'. The Great Pyramid's 'magic' multiplication number is 43,200,⁴ whereas the magic number for the Atlant Pyramid is 4,320 (smaller by a factor of 10, as it is 10 times the Great Pyramid's size).

These dimensionally encoded architectural features confirm the builders of the Orion Pyramid Complex at Giza, Egypt used the Atlant Pyramid (situated above sea level at that time) as a 10:1 scale model for the Great Pyramid. According to information imparted through the Plejaren ET contacts of Swiss farmer Eduard Meier, the founding of Atlantis took place approximately 133,000 years ago, through colonization efforts of the Plejaren leaders Atlant and Karyatide, from the planet Erra of the Plejares system.

This primary period of the Atlantean civilization on Earth progressed from its founding ~133,000 bp up until ~52,300 bp, when the Atlant Pyramid subsided far below sea level during the first destruction of Atlantis. This event coincided with the mega-eruption of Maninjau Volcano in Padang, Sumatra.⁵ The same Plejaren ET visitors have also given the construction date of the Orion Pyramid Complex of present-day Giza, Egypt at ~73,350 bp. According to these construction dates, the Atlant Pyramid and the Great Pyramid would have functioned simultaneously for ~21,000 years, driving a major expansion period in both Atlantis and Europe.



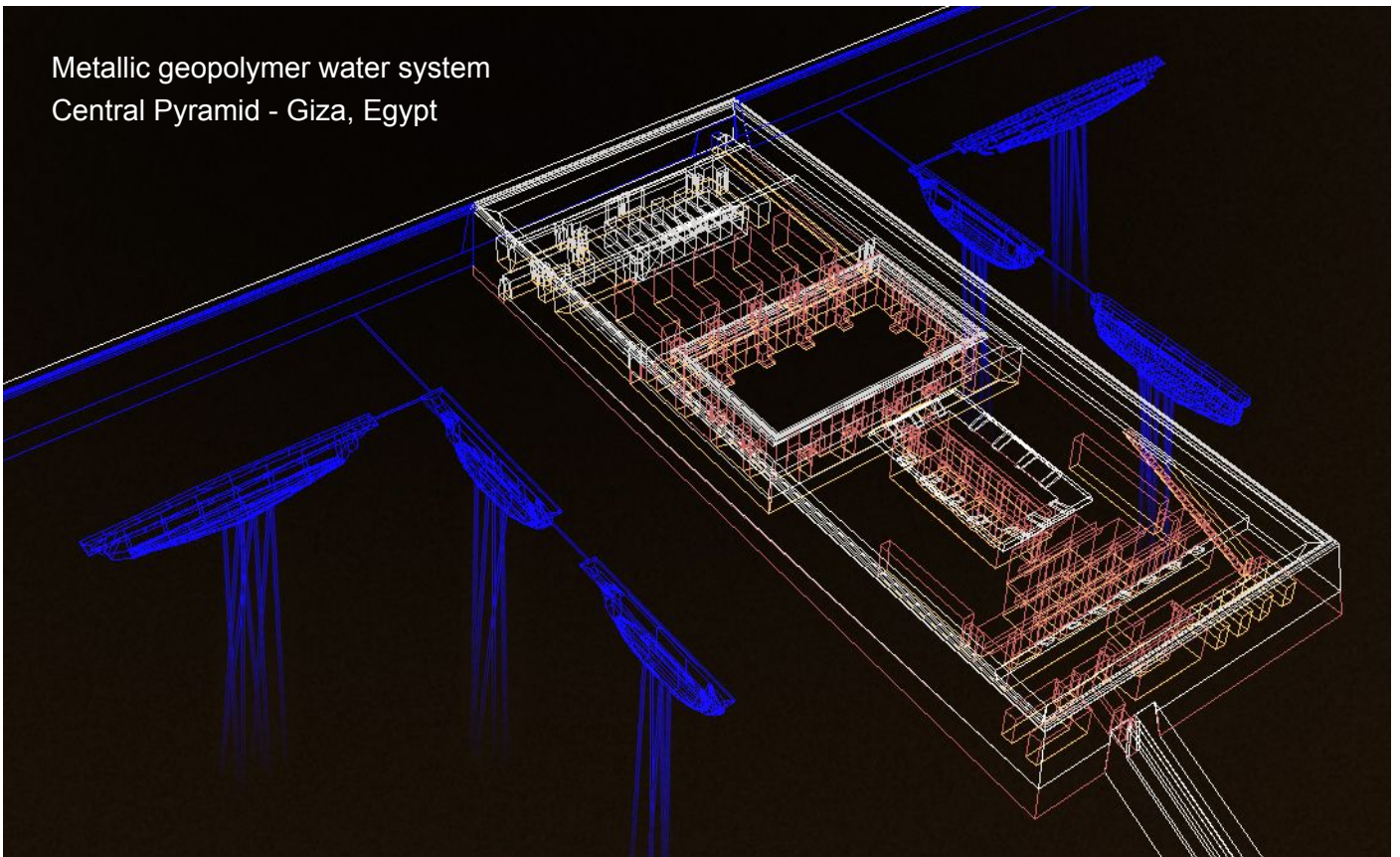
All but the top of the Atlant Pyramid remains buried under hundreds of feet of lava that were deposited at the time of its catastrophic submergence below the Atlantic Ocean. The remnants of huge, flat-topped buildings which have not been covered in volcanic deposits can be observed at the base of Blake Escarpment (above). Future investigations of this site will provide high-resolution bathymetry data and geopolymer stone samples.

At the time of its construction at ~133,000 bp, the Atlant pyramid was situated at the exact center of Earth's landmass above sea level. Relevant indications from other ancient underground cities dating to the same time period, marked by HHO plasma melt formations, archways and caves at Panther Beach, California; Cabo San Lucas, Mexico; Baigong Cave, China; and Yelhiu, Taiwan. The high-precision mathematical distribution pattern demonstrated by the relative geositions these advanced underground cave complexes conform to the global Atlantean pyramid network, efficiently transducing planetary infrasound resonance.

Specialized drinking water purification systems were constructed around each of the pyramids, with water channels feeding a series of long, rectangular pools covered by limestone blocks. These pools were lined with colorful geopolymer sandstone loaded with an assortment of metallic oxide particles that display much greater hardness than both the natural limestone bedrock and artificial limestone megaliths of the temples.



Metallic geopolymer water system
Central Pyramid - Giza, Egypt



Metallic geopolymer trough
Central Pyramid - Giza, Egypt



Large areas of metallic geopolymer stone was mined from the foundations of a series of water troughs that surrounded temple buildings on the eastern side of the Central Pyramid, which was known as the 'Temple of Sacrifice' during the reconstruction period ~30,000 years ago. According to the detailed Life Readings of Edgar Cayce, this rebuilding process was completed by King Arart, as directed by Hermes and Ra-Ta.

Extensive damage has been incurred by successive mining activities undertaken by many generations of builders in this area, due to the very high content of particulate metals present in these unusual, melted geopolymer sandstone deposits lining the Orion Pyramids' original drinking water purification system.

Despite extensive damage from extractive mining, low sidewalls of the pools are still partially intact (above), which were originally covered by a series of large limestone slabs, which can still be observed covering 4 of the 6 pools that surround the entry temple on the east side of the Central Pyramid on the Giza Plateau.

For decades, archeological data regarding significant traces of exotic metals incorporated into architectural features and geopolymer pool linings have been entirely suppressed by government 'Egyptologists' and reinforced by academia all over the world. Research findings on this subject were first obtained in the 1980s, yet have only recently been strategically disclosed to the general public through the ISIDA Project, whose satanic affiliation is blatantly advertised by an illuminati-style logo design with Masonic square and compass.

Trace element studies privately conducted over the past decade by the Russian-based counter-intelligence group reveal the presence of blends of exotic metallic particles that include strontium (Sr), barium (Ba), cerium (Ce), dysprosium (Dy) and lanthanum (La), as well as radioactive elements such as samarium (Sm), vanadium (V), europium (Eu), gadolinium (Gd), neodymium (Nd), thorium (Th) and uranium (U).⁶ The bulk of the geopolymeric materials consist of sodium-aluminosilicate cements with iron (Fe) and manganese (Mn) oxides, cast in aqueous mixtures of calcined orange kaolin clay and sodium hydroxide (NaOH).



Their bright coloration brings immediate attention to the iron-rich oxide formations surrounding the main pyramids at Giza. The false assumptions of geologists who routinely identify these metallic formations as natural ores are exposed by simply metering the high radioactivity of the material using a Geiger counter.



The abundance of exposed surface features presenting metallic sandstone geopolymers reveals that the Orion Pyramids, and the entire Giza Plateau, contains veins of *hundreds of tons of metallic geopolymers* that include many radioactive elements that are fully disregarded by the entire field of so-called 'experts'.



Local tour guide Yusef Awyan points out a variety of iron oxide formations on the Giza Plateau, in front of the Central Pyramid and filling in seams between megalithic blocks forming the Sphinx causeway (below).⁷ Fragments sampled from these dark red-brown geopolymer sandstone veins have identified a variety of exotic metals that do not occur together in nature, but must have been mined at several different locations before having been refined, pulverized and blended together as oxide powders for casting.



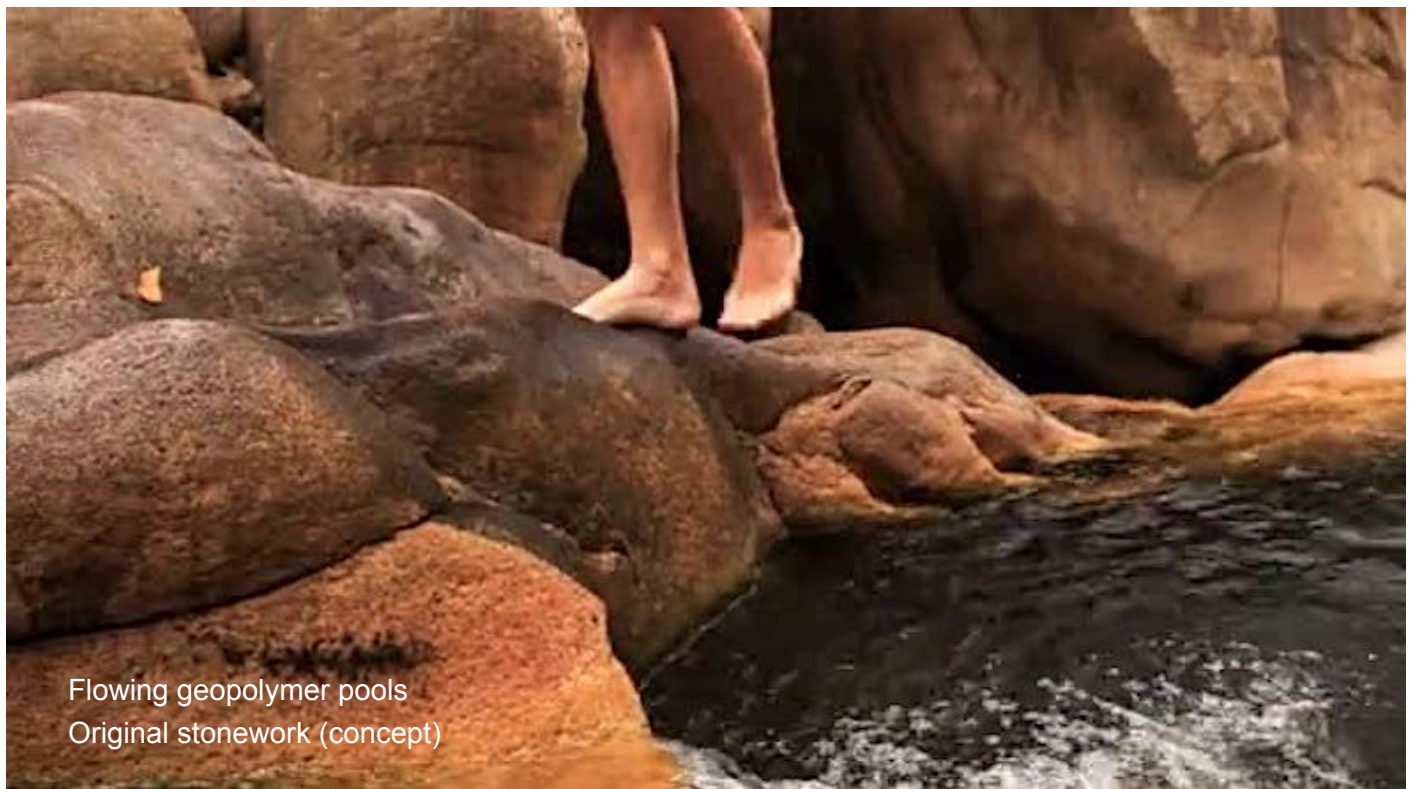
Metallic oxide vein
Central Pyramid - Giza, Egypt



The only exception to this unwritten rule in academic Egyptology is the ISIDA Project, which has been fully authorized by the Egyptian antiquities authority to collect samples from various locations on the Giza Plateau and from within the various ancient temple structures in the region. The reason for exclusive access having been granted to the ISIDA Project becomes clear after a thorough review of their process and conclusions.

Supposed 'control samples' tested by the ISIDA group have been falsely designated as natural materials when their own analyses indicate the presence of the same exotic trace metals found in the other samples tested. Chemical analyses published by the ISIDA Project were shared exclusively through US government disinformation agent Geoffrey Drumm, whose fanaticism aims to cloak the subject in ridiculous hypotheses.

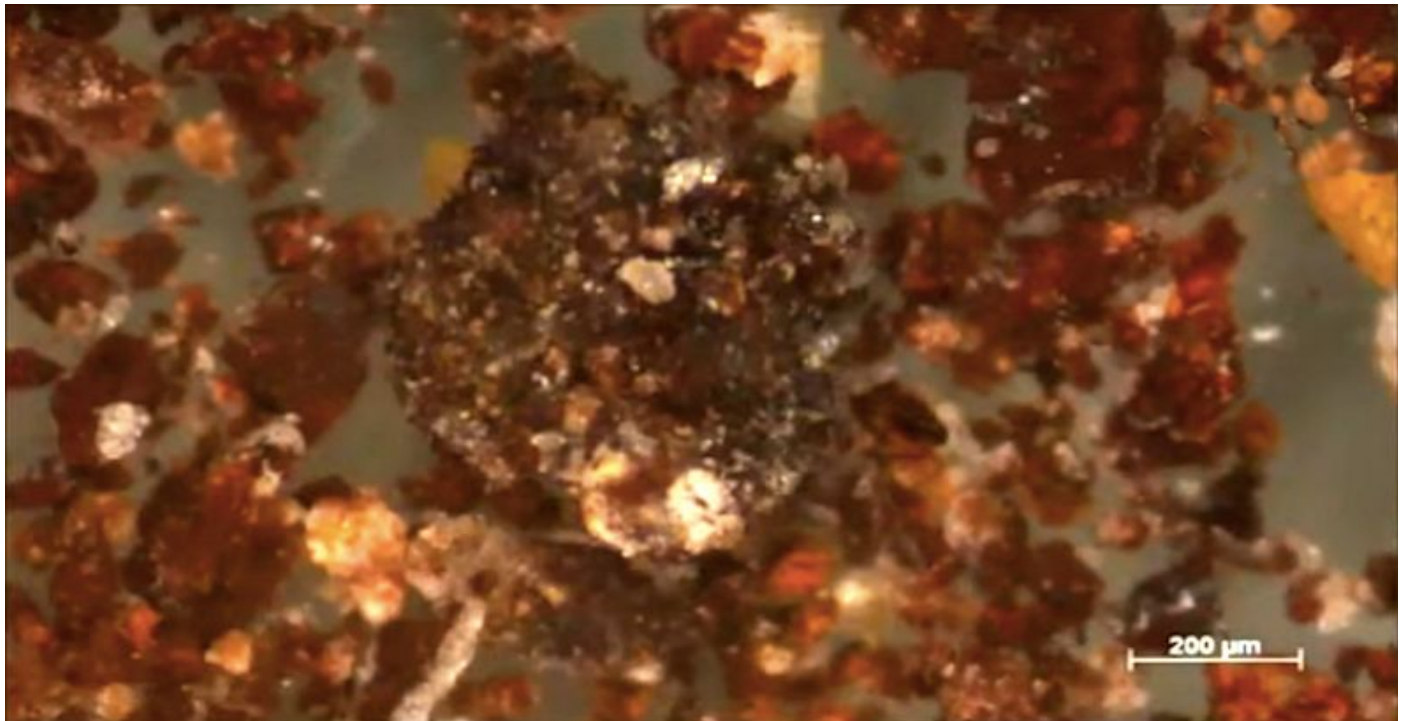
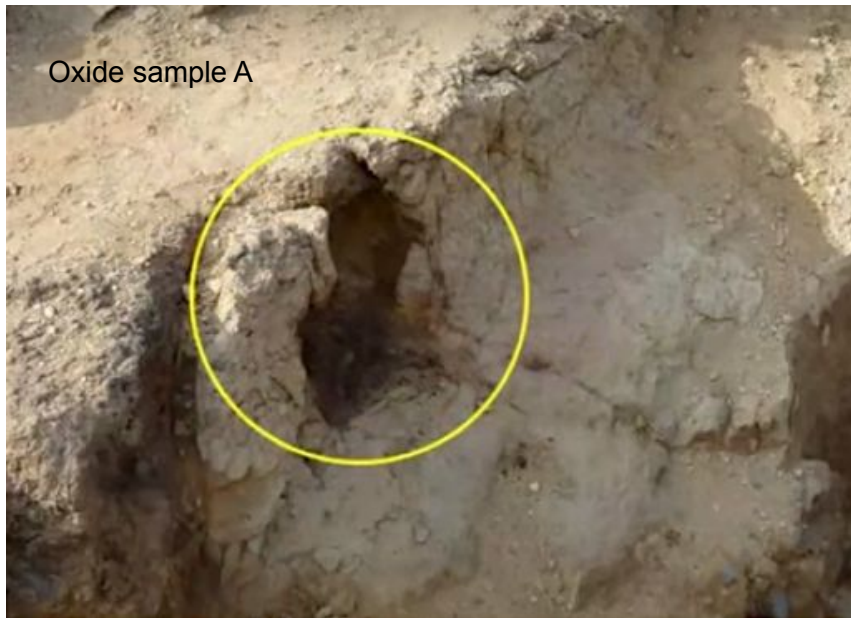
By contrast, an *accurate reassessment* of relevant chemical analyses of metallic geopolymers from the Giza Plateau is given here, revealing the pyramid builders' selective inclusion of exotic metals possessing many radionuclides of various types. Purposeful applications of trace inclusions within architectural features about the plateau were made for delivering ionizing radiations of every kind *for vitalizing human bodies at the site*.



The original appearance of the Orion Pyramid Complex included large, flowing areas of brightly colored metallic geopolymer formations that were damaged during a series of cataclysmic events that befell the civilization of Atlantis over tens of thousands of years. There were at least 3 major reconstruction periods that were undertaken after destructive periods had passed, including the Great Flood event estimated at 30,245 b2k according to ice core chronologies established from various depositions in polar regions.⁸

Sequential phases of pyramid reconstruction and calamity took place over such great time scales that can be attributed to different levels of technological capabilities, which progressively diminished through the course of each era of civilization. Geopolymer restoration work was accomplished during the Dynastic Egyptian period using hand-mixing and hand-casting methods, *whereas earlier periods used vimana craft*.

A hand sample of black material embedded in limestone was obtained from pits representing remnants of water purification and sterilization pools of the Central Pyramid's Causeway Temple (overleaf). Results from chemical analysis given in grams per ton (g/t) showed the black geopolymer sample A primarily consists of aluminum (Al), iron (Fe), manganese (Mn), calcium (Ca), gypsum (calcite) and sodium (Na), with particulate inclusions of a wide variety of exotic metals that imbue the material with specialized magnetic properties.



Trace elements, g/t

Be	sc	V	Cr	co	Ni	Cu	Zn	Ga	Rb	Sr	Y	Zr	Nb	Mo	Cs	Ba	La
4.89	0.44	373.26	9.40	111.07	214.18	4.26	105.03	0.73	0.91	337.55	19.41	5.60	0.50	35.17	0.06	85.83	6.74

Ce	Pr	Nd	sm	Eu	Gd	Tb	Dy	Ho	Er	Tm	Yb	Lu	hf	Pb	Th	U
9.54	1.45	7.79	1.41	0.39	2.85	0.36	2.51	0.56	1.79	0.21	1.29	0.20	0.16	1.72	0.34	13.05

A large hand sample of a bright orange-red geopolymer material was removed from an outcropping of highly weathered limestone bedrock near the pit excavations (opposite), presenting a very similar trace element composition with elevated levels of strontium (Sr) and barium (Ba) oxides (above). The macro-elemental composition reveals yellow and red iron oxides (Fe_2O_3) with manganese oxide (MnO) suspended in sodium-aluminosilicate geopolymer. The composite is cast from aqueous mixtures of sodium hydroxide (NaOH) and calcined kaolin clay, as replicated by Dr. Davidovits of the Geopolymer Institute in Saint-Quentin. France.



Oxide sample B



Trace elements, g/t

Be	sc	V	Cr	co	Ni	Cu	Zn	Ga	Rb	Sr	Y	Zr	Nb	Mo	Cs	Ba	La
2.18	0.40	263.37	21.43	139.60	171.90	3.94	367.14	2.12	1.34	1351.15	39.32	3.07	0.38	44.74	0.08	537.11	12.38

Ce	Pr	Nd	sm	Eu	Gd	Tb	Dy	Ho	Er	Tm	Yb	Lu	hf	Pb	Th	U
18.02	2.83	15.44	3.21	0.93	6.46	0.79	5.36	1.15	3.42	0.37	2.22	0.33	0.17	1.56	0.32	17.92



Oxide sample C



Trace elements, g/t

Be	sc	V	Cr	co	Ni	Cu	Zn	Ga	Rb	Sr	Y	Zr	Nb	Mo	Cs	Ba	La
3.45	2.35	169.69	55.91	108.69	241.06	0.00	169.25	1.07	1.10	1813.60	38.61	5.57	0.50	20.67	0.08	527.19	45.03

Ce	Pr	Nd	sm	Eu	Gd	Tb	Dy	Ho	Er	Tm	Yb	Lu	hf	Pb	Th	U
43.26	7.11	33.30	5.93	1.53	8.94	1.16	7.42	1.43	4.30	0.50	3.24	0.45	0.22	1.48	0.33	11.65



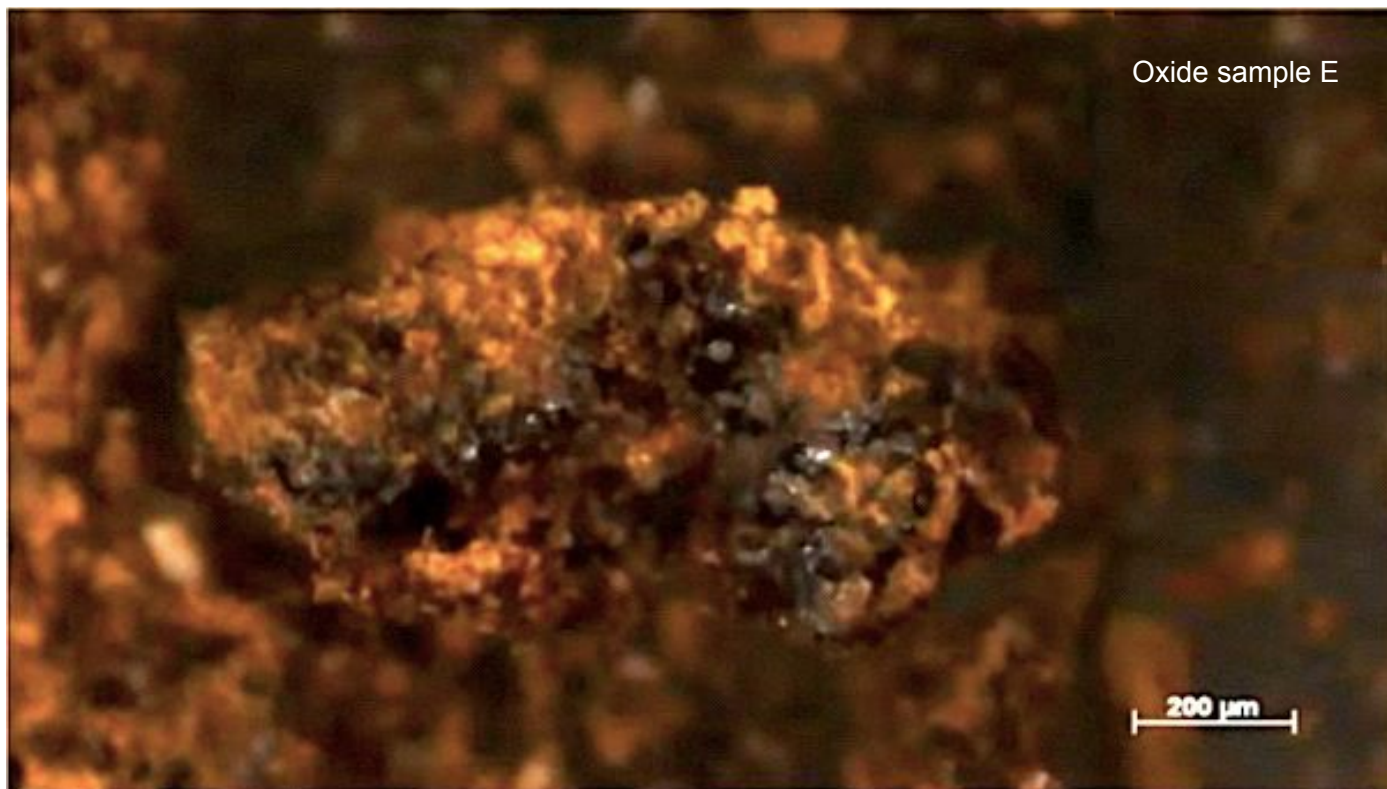
Oxide sample D

Trace elements, g/t

Be	sc	V	Cr	co	Ni	Cu	Zn	Ga	Rb	Sr	Y	Zr	Nb	Mo	Cs	Ba	La
11.54	1.13	229.94	44.31	112.22	320.09	2.98	813.86	2.36	1.89	1046.12	186.43	6.34	0.61	15.53	0.14	60.07	51.69

Ce	Pr	Nd	sm	Eu	Gd	Tb	Dy	Ho	Er	Tm	Yb	Lu	hf	Pb	Th	U
207.49	31.47	160.36	38.66	9.85	47.16	6.10	37.08	6.51	19.24	2.36	16.37	2.15	0.65	2.70	0.83	57.46

Oxide sample E



Trace elements, g/t

Be	sc	V	Cr	co	Ni	Cu	Zn	Ga	Rb	Sr	Y	Zr	Nb	Mo	Cs	Ba	La
3.97	1.13	167.28	43.42	93.82	220.92	11.34	341.09	1.01	0.90	103.67	60.00	3.91	0.36	5.78	0.07	27.14	14.86

Ce	Pr	Nd	sm	Eu	Gd	Tb	Dy	Ho	Er	Tm	Yb	Lu	hf	Pb	Th	U
64.87	4.82	26.55	7.28	2.10	11.64	1.71	11.65	2.27	7.04	0.92	6.48	0.88	0.22	2.09	0.25	14.29

Oxide sample F



Trace elements, g/t

Be	sc	V	Cr	co	Ni	Cu	Zn	Ga	Rb	Sr	Y	Zr	Nb	Mo	Cs	Ba	La
2.77	0.69	278.39	23.87	103.76	279.30	3.75	361.33	1.40	1.60	269.64	82.40	5.01	0.60	13.94	0.12	270.11	25.98

Ce	Pr	Nd	sm	Eu	Gd	Tb	Dy	Ho	Er	Tm	Yb	Lu	hf	Pb	Th	U
94.82	11.22	62.15	14.47	3.79	19.26	2.55	16.06	3.04	9.08	1.09	7.23	0.99	0.35	1.60	0.47	22.15



Oxide sample G

Trace elements, g/t

Be	sc	V	Cr	co	Ni	Cu	Zn	Ga	Rb	Sr	Y	Zr	Nb	Mo	Cs	Ba	La
2.52	1.25	267.92	50.17	91.07	186.76	1.73	291.18	1.88	1.76	191.94	213.56	4.03	0.49	11.25	0.09	200.98	77.02
Ce	Pr	Nd	sm	Eu	Gd	Tb	Dy	Ho	Er	Tm	Yb	Lu	hf	Pb	Th	U	
204.76	19.27	98.49	21.23	6.03	36.83	4.91	32.45	6.49	19.49	2.31	14.92	2.08	0.52	0.74	0.29	57.27	



Oxide sample H

Trace elements, g/t

Be	sc	V	Cr	co	Ni	Cu	Zn	Ga	Rb	Sr	Y	Zr	Nb	Mo	Cs	Ba	La
1.82	2.81	17.99	41.39	3.70	7.47	3.21	55.79	11.24	56.70	145.99	15.61	176.37	7.91	1.81	0.59	470.37	33.95
Ce	Pr	Nd	sm	Eu	Gd	Tb	Dy	Ho	Er	Tm	Yb	Lu	hf	Pb	Th	U	
72.08	8.19	35.93	6.05	1.00	6.08	0.67	3.77	0.65	2.13	0.27	1.97	0.28	4.20	8.89	4.54	1.63	

The combination of exotic metal oxide compounds indicated by electron microscopy results of the ISIDA Project have not been adequately characterized by that group, and conform to a very specific class of compounds that are often applied in today's electronic devices for specific functions as ceramic composites. Metal/ceramic powder composites are widely applied today in the production of *strontium ferrite* magnets containing magnetite (Fe_3O_4), giving these materials their characteristic dark grey coloration. Permanent magnets of this type find common uses in flexible magnet strips, loud speakers and small electric motors.

The same elements found in the Giza metallic geopolymer samples are often applied in modern industrial electronics as ferrites of various types, listed here with elemental compositions and technical applications:

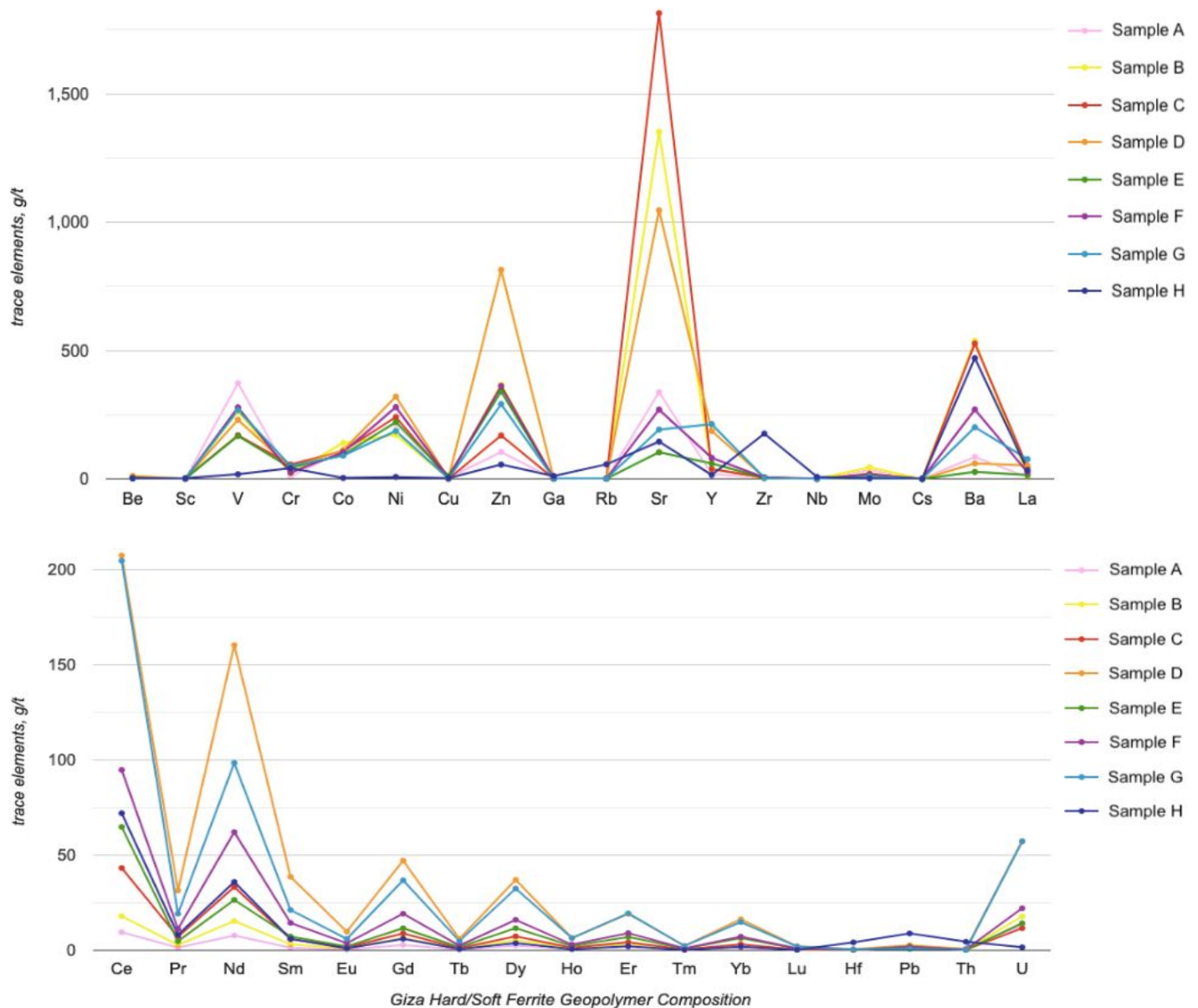
- Hard ferrites - Strontium ferrite ($\text{SrO} \cdot 6\text{Fe}_2\text{O}_3$), ($\text{SrO} \cdot 6\text{Fe}_3\text{O}_4$) used in microwaves, recording, magneto-optics
 - Barium ferrite ($\text{BaO} \cdot 6\text{Fe}_2\text{O}_3$) used in magnets, loudspeakers, magnetic recording strips
- Semi-hard ferrites - Cobalt ferrite (CoFe_2O_4) used in sensors actuators, transducers
 - Cobalt-erbium ferrite ($\text{Co}_{(1-a)}\text{Er}_a\text{Fe}_2\text{O}_4$) used in magnetic diagnostics, drug delivery, catalysis
 - Cobalt-yttrium ferrite ($\text{Co}_{(1-a)}\text{Y}_a\text{Fe}_2\text{O}_4$) used in microwaves, magnetic sensors, actuators
 - Cobalt-zirconium ferrite ($\text{Co}_{(1-a)}\text{Zr}_a\text{Fe}_2\text{O}_4$) used in high-density recording devices, drug delivery
 - Cobalt-dysprosium ferrite ($\text{Co}_{(1-a)}\text{Dy}_a\text{Fe}_2\text{O}_4$) used in catalysis
 - Cobalt-cerium ferrite ($\text{Co}_{(1-a)}\text{Ce}_a\text{Fe}_2\text{O}_4$) used in resistance switching recording devices
 - Cobalt-samarium ferrite ($\text{Co}_{(1-a)}\text{Sm}_a\text{Fe}_2\text{O}_4$) used in high-temperature generators, pumps
- Soft ferrites - Nickel-copper ferrite ($\text{Ni}_a\text{Cu}_{(1-a)}\text{Fe}_2\text{O}_4$) used in magnetic materials, magnetic sensors
 - Nickel-thulium ferrite ($\text{Ni}_a\text{Tm}_{(1-a)}\text{Fe}_2\text{O}_4$) used in ceramic magnets of microwaves
 - Nickel-zinc ferrite ($\text{Ni}_a\text{Zn}_{(1-a)}\text{Fe}_2\text{O}_4$) used in transformer cores for RF frequencies >1 MHz
 - Nickel-zinc-thorium ferrite ($\text{Ni}_a\text{Zn}_{(1-a)}\text{Fe}_2\text{O}_4\text{Th}_a$) used in high-speed switching recording devices
 - Manganese-zinc ferrite ($\text{Mn}_a\text{Zn}_{(1-a)}\text{Fe}_2\text{O}_4$) used in transformer cores for frequencies <5 MHz
 - Manganese-chromium ferrite ($\text{Mn}_a\text{Cr}_{(1-a)}\text{Fe}_2\text{O}_4$) used in high-speed switching recording devices
 - Niobium-titanium-molybdenum ferrite ($\text{Nb}_a\text{Ti}_{(1-a)}\text{Fe}_2\text{O}_4\text{Mo}_a$)
 - Zinc ferrite (ZnFe_2O_4) used in pigments requiring high heat stability
 - Zinc-dysprosium ferrite ($\text{Zn}_{(1-a)}\text{Dy}_a\text{Fe}_2\text{O}_4$) used in biosensors, high-density recording devices, drug delivery, catalysis, magneto-optical devices
 - Gadolinium ferrite (GdFe_2O_4) used in high-density recording devices, quantum computation, drug delivery, MRI imaging contrast agents
 - Praseodymium ferrite (PrFe_2O_4) used in high-density recording devices
 - Samarium ferrite (SmFeO_3) used in gas sensors, solid oxide fuel cell cathodes, catalysis
 - Holmium ferrite (HoFe_2O_4)
 - Cerium ferrite (CeFe_2O_4)
 - Lutetium ferrite (LuFe_2O_4)
 - Lanthanum-cerium ferrite ($\text{LaCeFe}_2\text{O}_4$) used in supercapacitors
 - Zirconium ferrite (ZrFe_2O_4) used in metal ion removal from waste water, drug delivery
 - Vanadium ferrite (VFe_2O_4) used in magnetic sensors, electrochemical capacitors, catalysis
 - Yttrium ferrite (YFe_2O_4) used in plastics, coatings, textiles, optical filters, catalysis
 - Erbium ferrite (ErFe_2O_4)

All ferrite composites are ferrimagnetic, showing the high coercivity associated with magnetization and attraction to magnets. Ferrite geopolymers were originally cast at Giza in long veins, radiating away from the pyramids through the piezoelectric limestone bedrock, for generating magnetically-driven ferroelectricity in the water systems and causeway pavements due to the coupling of inhomogenous order parameters.

Inclusion of multiple ferrite types in geopolymer composite materials combines desirable properties of hard, semi-hard and soft classes for bioelectrification by barefoot ambulation on walkway pavements. These elements were selectively applied in castable ferrite sodium-silicate geopolymers for lowering energy losses and eddy currents that arise during EM coupling of magnetic and electric fields. This special effect greatly increases the breadth of toroidal EM fields that encompass each of the 3 pyramids of the Orion Complex.

A compilation of test results for Giza ferrite geopolymer samples A through H are presented in a pair of line graphs (opposite), obtained from various sampling sites around the Central Pyramid's Causeway Temple:

Long-lived radio-isotope traces of several elements are used today for tuning and enhancing the properties of diverse ferrite materials, especially rubidium (Rd^{87}), zirconium (Zr^{96}), molybdenum (Mo^{100}), barium (Ba^{130}), lanthanum (La^{138}), neodymium (Nd^{144} , Nd^{150}), samarium (Sm^{147}), europium (Eu^{151}), gadolinium (Ga^{152}), hafnium (Hf^{174}) and lutetium (Lu^{176}). Even radioactive isotopes of toxic elements such as thorium (Th^{232}) and uranium (U^{235} , U^{238}) have been safely applied for several decades as trace oxides in industrial ferrites for improving high-speed switching in magnetic devices by inhibiting the motion of domain walls.⁹



These comprehensive findings confirm the presence of architectural features cast with traces of *long-lived radionuclides* that still emit potent decay radiations of all kinds –being just as emissive in the present-day as they were at the time of their casting. When used in modern electronics as ceramic composites the quantity of radiation emitted by devices is negligible, due to the small size of ferrite components. In contrast, when multi-ferrite geopolymer water systems and walkway pavement coatings are applied on a monumental scale at pyramids and underground temples such as the Orion Pyramid Complex, *radiation exposures increase*.

The great significance of the geopolymeric blending of exotic metal powders has been marginalized and mischaracterized by the ISIDA Project and all other investigators of the Orion Pyramid Complex on the Giza Plateau. The present identification of multi-ferrite geopolymers represents a major breakthrough in our understanding of bioelectrical, biophotonic and psychoacoustic functions of the world's pyramid network.

Main isotopes ^[1]			Decay	
	abundance	half-life ($t_{1/2}$)	mode	product
⁸⁷ Rb	27.8%	4.97×10^{10} y	β^-	⁸⁷ Sr
⁹⁶ Zr	2.80%	2.0×10^{19} y	β^-	⁹⁶ Mo
¹⁰⁰ Mo	9.74%	7.1×10^{18} y	β^-	¹⁰⁰ Ru
¹³⁰ Ba	0.11%	2.7×10^{21} y	ϵ	¹³⁰ Xe
¹³⁸ La	0.089%	1.05×10^{11} y	ϵ	¹³⁸ Ba
			β^-	¹³⁸ Ce
¹⁴⁴ Nd	23.8%	2.29×10^{15} y	α	¹⁴⁰ Ce
¹⁴⁷ Sm	15%	1.06×10^{11} y	α	¹⁴³ Nd
¹⁵⁰ Nd	5.60%	6.7×10^{18} y	β^-	¹⁵⁰ Sm
¹⁵¹ Eu	47.8%	5×10^{18} y	α	¹⁴⁷ Pm
¹⁵² Gd	0.2%	1.08×10^{14} y	α	¹⁴⁸ Sm
¹⁷⁴ Hf	0.16%	7.0×10^{16} y	α	¹⁷⁰ Yb
¹⁷⁶ Lu	2.60%	3.78×10^{10} y	β^-	¹⁷⁶ Hf
²³² Th	100.0%	1.4×10^{10} y	α	²²⁸ Ra
²³⁵ U	0.72%	7.04×10^8 y	α	²³¹ Th
			SF	–
²³⁸ U	99.3%	4.468×10^9 y	α	²³⁴ Th
			SF	–
			β^-	²³⁸ Pu

The variety of exotic metal elements with long-lived radio-isotopes applied as admixtures in the Giza geopolymer ferrite veins are presented with half-life durations (at left). These metastable isotopes include radionuclides of many decay types, emitting ionizing radiation in the form of high-energy α -particles, γ -rays, neutrinos and electrons. Relative values for natural abundance provide nominal percentages for each isotope, as compared with the percentages of other stable or metastable isotopes of the same element.

Acute chemical toxicity of many metastable elements limits their internal application in rasayana elixir preparations to nano-doses, having instead been applied in architectural features of monumental temples during the Atlantean Era of high civilization. Edgar Cayce identified the use of elements for mental projection and quantum teleportation by the giant leader of Atlantis, named 'Amilius' (Readings 364-3, -4, -7):

In the period, then –some hundred, some 98,000 years before the entry of Ram into India– there lived in this land of Atlantis one Amilius, who had first noted that of the separations of the beings as inhabited that portion of the Earth's sphere or plane of those peoples into male and female as separate entities, or individuals. As to their forms in the physical sense, these were much rather of the nature of thought forms, or able to push out of themselves in that direction in which its development took shape in thought...

In these things, then, did Amilius see the beginning of, and the abilities of, those of his own age, era, or period, not only able to build that as able to transpose or build up the elements about them but to transpose them bodily from one portion of the universe to the other, through the uses of not only those recently re-discovered [HHO] gases, and those of the electrical and aeriatic formations –in the breaking up of the atomic forces to produce impelling force to those means and modes of transposition, or of travel, or of lifting large weights, or of changing the faces or forces of nature itself...

In the material world we find there is in the mineral kingdom those elements that are of the nature as to form a closer union one with another, and make as for compounds as make for elements that act more in unison with, or against... the Earth's force, as makes for those active forces in the elements that are about the Earth. Such as we may find in those that make for the active forces in that of uranium... for the rates of emanation as may be thrown off from same. So, as illustrated in the union, then, of –in the physical compounds– that as may vibrate, or make for emanations in the activities of their mental and spiritual, and material, or physical forces, as may make for a greater activity in this Earth environ. Then, there may be seen that as is in an elemental, or compound, that makes for that as is seen in the material experience as to become an antipathy for other elements that are as equally necessary in the experience of man's environ as in the combination of [HHO] gases as may produce whenever combined that called water, and its antipathy for the elements in combustion is easily seen... in man's experience.

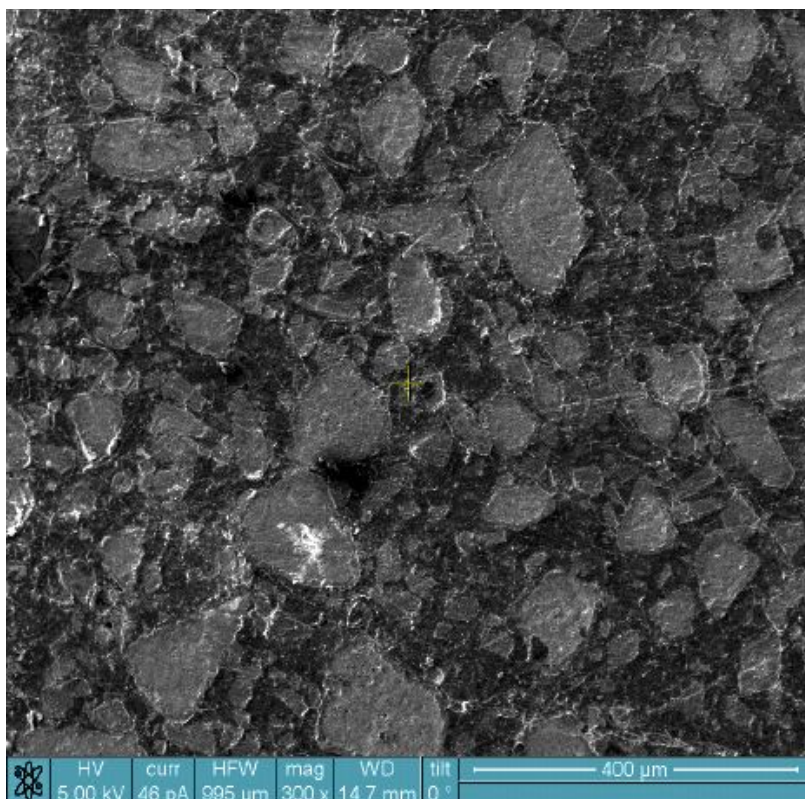
So in those unions of that in the elemental forces of creative energies that take on the form... of man or woman, with its natural or... elemental forces of its vibration, with the union of two that vibrate or respond to those vibrations in self, create for that ideal that becomes as that, in that created, in the form –as is known as radium, with its fast emittal vibrations, that brings for active forces, principles, that makes for such atomic forces within the active principles of all nature in its active force as to be one of the elemental bases from which life in its essence, as an active principle in a material world, has its sources, give off that which is ever good –unless abused, see? So in that may there be basis for those forces, as has been, as is sought, thought, or attained by those who have, through the abilities of the vibrations, to make for a continued force in self as to meet, know, see, feel, understand, those sources from which such begets that of its kind...

The compelling holism of such complex explanations given by Cayce during Life Readings in the 1930s is simply remarkable, and requires advanced scientific knowledge to even grasp the concept being conveyed. The present findings of ferrite geopolymers distributed throughout the Orion Pyramid Complex represent indisputable archeological evidence for the extraordinary statements made by Cayce regarding the highest applications of metallic compounds *for attaining the innate human capability for quantum teleportation*.

Indirect references are made to the active forces emitted by photoluminescent radium compounds (RaS), effectively illuminating the cells of the human body with photons in the form of y-rays and visible light rays. By this means, the human body acquires the same special properties exhibited by the synthetic temple stonework; *making a temple of the body through which the Divine spirit of light can fully manifest*.

Radiant architectural features reflect the alchemical formulations ingested by Siddha adepts in India, whose vast knowledge was passed down to them from the living descendants of Atlantean subterranean societies that include cities at Mount Meru, Mount Kailash, Agharta- α , Agharta- β , Shambhala and Kalapa.

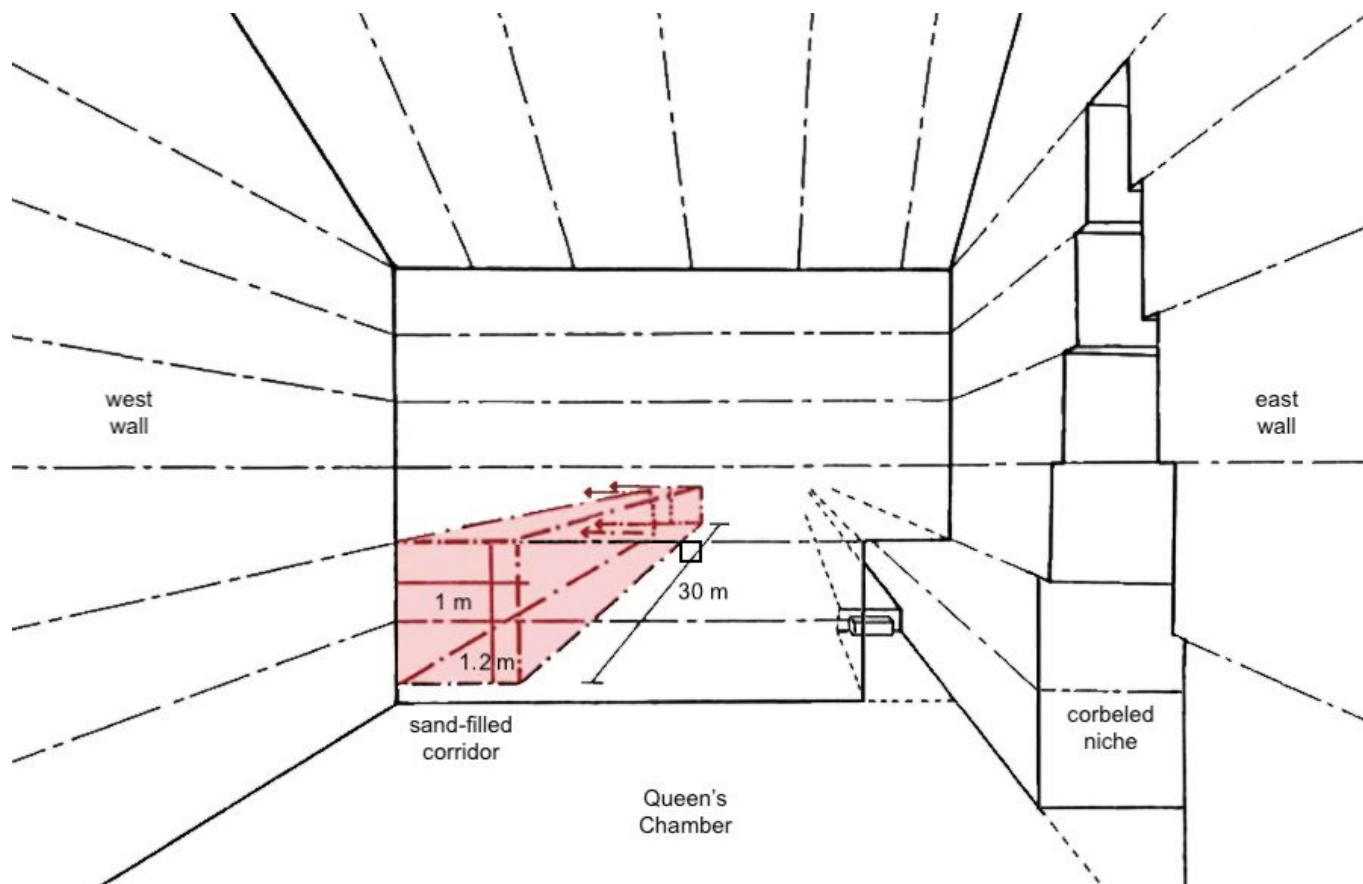
Traditional Sanskrit practices involving biophotonic (internal) and metallurgic (external) forms of alchemy are considered prerequisite knowledge for activating the latent powers by yoga, pranayama, mantra and meditation –through which the siddhis, or *attainments* become fully engaged. Among the most advanced arts belonging to this class of quantum biological capabilities are those of levitation and teleportation.



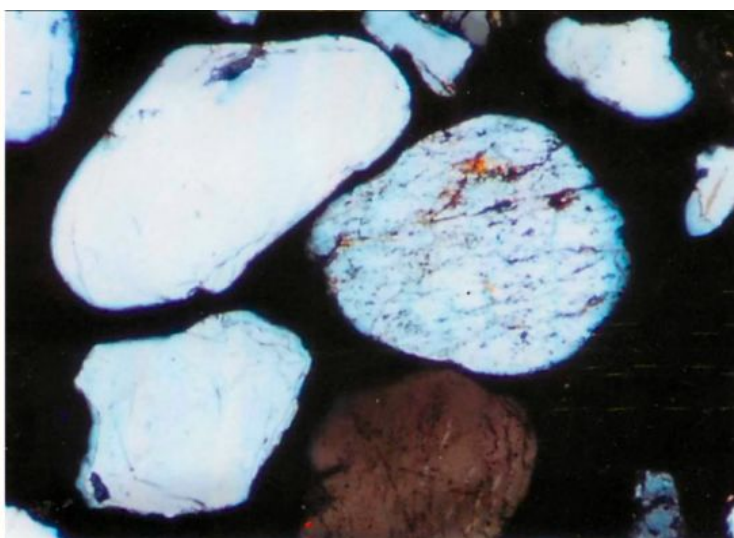
Ingestion of RaS bhasma reflects the complimentary application of specialized ferrite materials in the construction of levitation galleries with curved walls or corbeled ceilings. A flexible, natural rubber-barium ferrite nanocomposite material was recently produced in 2012¹⁰ (SEM image, at left) after having been previously developed tens of thousands of years ago by Atlantean metamaterials inventors and applied by architectural engineers at subterranean cities that include Tatra Pyramid Complex in present-day Slovakia. In 1944, toward the end of World War II, soldier Antonin Horak surveyed a limestone cave system to find a crescent-shaped vertical levitation silo that could be entered through a large crack in the chamber's curved and inclined front wall. The durability and black coloration of a thick, rubber ferrite nanocomposite material forming the enormous curved walls of the levitation silo indicate a strontium-magnetite composition similar to those in development by modern scientific materials research.

In a related archeological discovery, hundreds of geopolymer granite discs presenting a cobalt-based semi-hard ferrite composition were discovered in the cave burials of the Dzopa Pyramid Complex in the Bayan-Har Mountains of China, now recognized as high-density recording devices. Cobalt ferrite (CoFe_2O_4) has been utilized in modern electronics for enhanced magnetoelectric effects by developing production methods involving the induction of a magnetic uniaxial anisotropy in ceramic composites by magnetic annealing.

The fact that the Bayan-Har cobalt ferrite discs incorporate this same data-recording material suggests they function as information storage devices that may preserve files from the Atlantean Era –*perhaps including video and audio content!* The Hall of Records spoken of by Edgar Cayce may contain digital storage files on hundreds of synthetic stone discs, in addition to large stone libraries of Paleo-Sanskrit hieroglyphic texts.



The original builders of the Orion Pyramids of Giza, Egypt also used radioactive materials for back-filling voids within the gigantic monuments. In 1986, Gilles Dormion sank 3 drill cores into the wall of the entry tunnel of the Queen's Chamber in the Great Pyramid, penetrating a void filled by monazite-quartz sands.¹¹ Drilling was discontinued and the findings effectively suppressed after their implications became clear; that a parallel hallway exists to the north of the Queen's Chamber passage, which has been back-filled (above).




Sand-filled corridors cannot be observed by muon scanning, but may be confirmed by metering and video observations using endoscopic cameras and radiation sensors that can be inserted through existing holes. Monazite contains high concentrations of rare elements that include cerium, neodymium, praseodymium, yttrium, thorium, silicon, aluminum and iron. These rare elements are present in monazite in the form of oxide compounds (P_2O_5 , Ce_2O_3 , La_2O_3 , Nd_2O_3 , Pr_2O_3 , Y_2O_3 , ThO_2) containing long-lived radio-isotopes.



The back section of the majestic corbeled niche recessed into the east wall of the Queen's Chamber (above) was vandalized by treasure hunters hundreds of years ago, by excavating a narrow tunnel for several meters before abandoning their toils. The excavation shows an orange layer of ferrite geopolymer was cast in between the rows of megalithic limestone blocks forming the chamber walls (below).



Ferrite cement filler
Queen's Chamber niche
Great Pyramid - Giza, Egypt



Ferrite-coated resonator box
Osiris Shaft - Giza, Egypt

Within the Osiris shaft, located below the Giza Plateau near the Central Pyramid of the Orion Complex, researchers have discovered rare metal inclusions in a fine coating deposited on the exterior surface of the dacite (fine-grained, red geopolymer granite) box. These fine metal particles include lead, titanium, arsenic, zinc and iron.¹² *Interior surfaces of the dacite box also display radioactive coatings that remain unpublished.*

Another original casting feature of the Giza Plateau was mined out of the Osiris Shaft chambers long ago, showing the same distinctive composition of a metallic geopolymer vein running in a planar, vertical position (opposite). Chemical analyses of similar samples obtained from surface features indicate the Osiris Shaft's metallic geopolymer veins are comprised of the same blend of long-lived radioactive oxide compounds.

The extreme size and depth of these hard, metallic stone features –*distributed throughout the interior, exterior and subterranean structures of the Orion Pyramid Complex*– represents very strong evidence for their purposeful construction by the original Paleo-Sanskrit builders of the site at ~73,350 years ago. Now, for the first time, the full significance of odd explanations given by Edgar Cayce can finally be recognized.

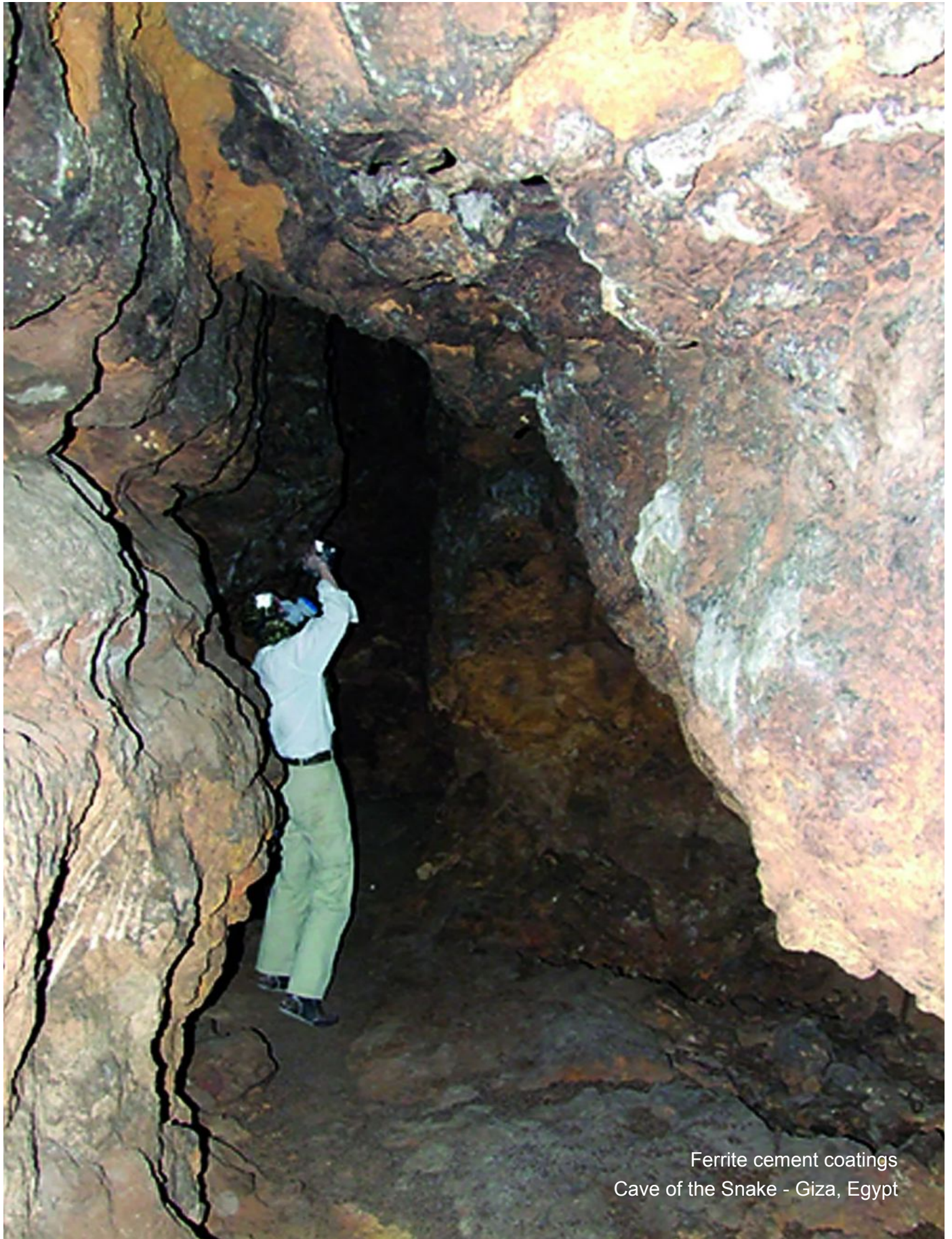
The same type of very hard, metallic sandstone geopolymer is found in the 'Cave of the Snake', accessed from the rear corner of the Tomb of the Birds (overleaf). Testing of rock samples obtained from these sites has never been reported by any investigators, nor has any radioactivity metering been documented there.



Ferrite cement veins
Osiris Shaft - Giza, Egypt

Tomb of the Birds
Giza, Egypt





Ferrite cement coatings
Cave of the Snake - Giza, Egypt

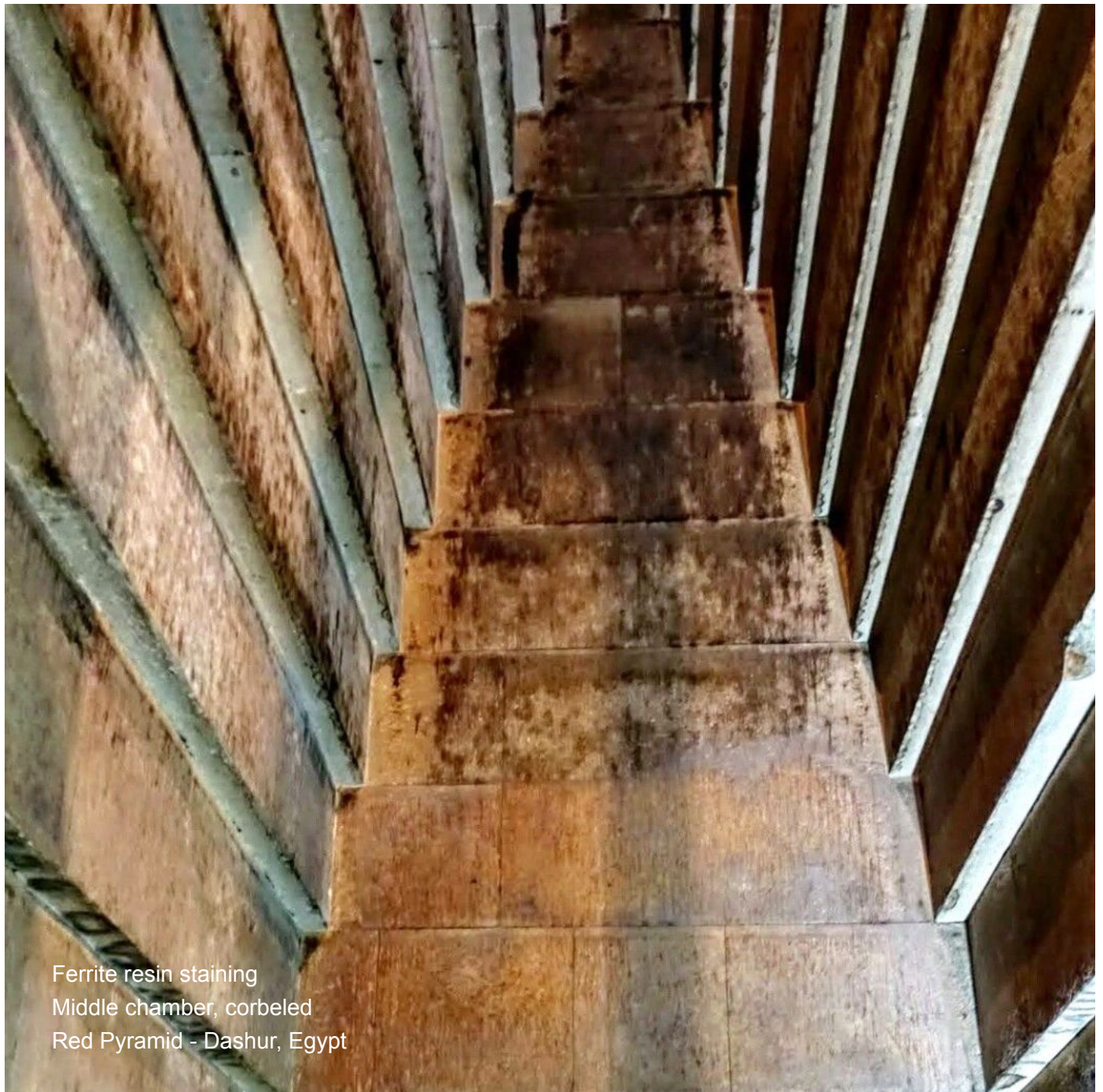


Ferrite cement sampling sites
Red Pyramid - Dashur, Egypt

The Red Pyramid of Dashur, Egypt has also been the recent subject of investigations by the ISIDA Project, known for its steeply angled passageways without any steps, designed with entry tunnels located high above ground level. These highly specialized architectural features reflect the same unusual design seen in the grand gallery of the Great Pyramid, also built without ascending steps, which indicates these spaces *were not designed for easy access by walking upright; serving instead as psychoacoustic levitation corridors.*



Corbeled ceilings of the Red Pyramid's inner chambers have been mapped by laser scanning techniques, applying the interior surface coloration to an exterior view of the chambers. The dark surface staining of the chamber walls is not observed within the connecting passages, having been unevenly painted on upper sections of the three chambers' high, stepped ceiling blocks.



Ferrite resin staining
Middle chamber, corbeled
Red Pyramid - Dashur, Egypt

Well-illuminated photographs of the interior of the third, uppermost chamber of the Red Pyramid display the accumulation of uneven applications of a dark brown, resin-like coating that had not been analyzed by any researchers on public records until the organized efforts of the ISIDA Project that began over a decade ago. Samples of this dark brown coating material were obtained and analyzed for their chemical composition.

Preferential treatments of the upper sections of the lofty chambers, while leaving the more accessible lower walls and connecting passages untouched, relates to the unusual function of the coatings that have not been properly identified until the present writing. Trace remnants of the same type of black chemical staining can be observed on the corbeled niche of the Queen's Chamber of the Great Pyramid, despite having been mostly removed long ago by conservators of the ancient monuments. The reason for this remains unclear, either having been done in ignorance of its ancient origin –or perhaps having been removed after it was determined to be the source of ionizing radiation exposures that were regarded as a hazard for tourists.

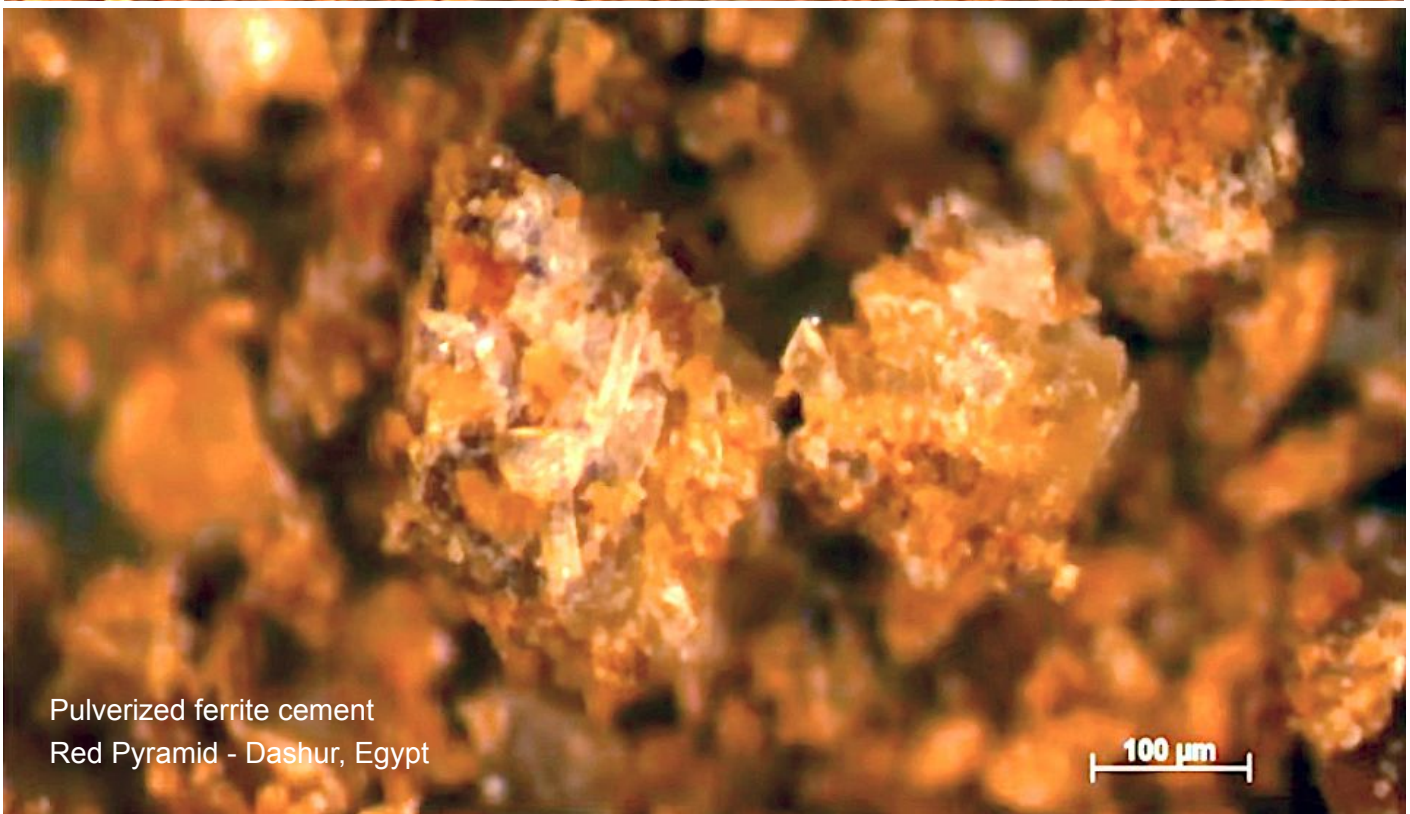
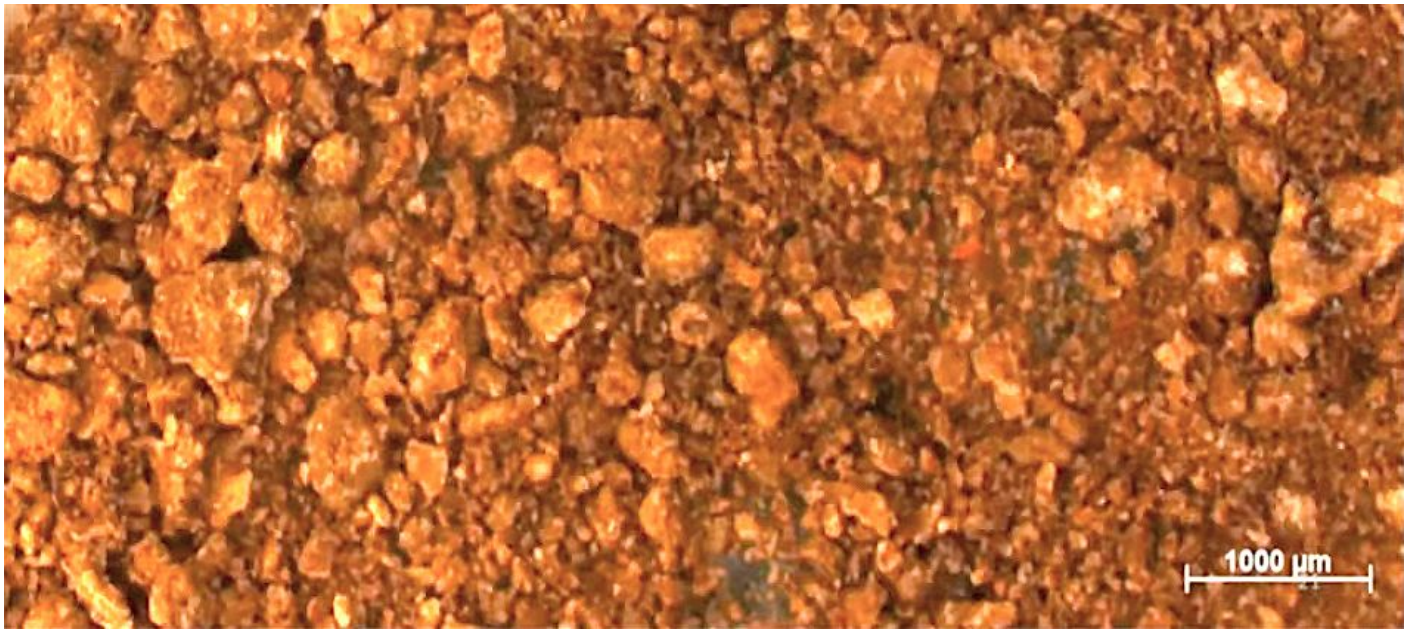
Microelement composition of the black substance, gram/ton								
Ce 1,26	Pr 0,15	Nd 0,68	Sm 0,13	Eu 0,03	Gd 0,17	Tb 0,02	Dy 0,14	
Ho 0,03	Er 0,08	Tm 0,01	Yb 0,07	Lu 0,01	Hf 0,11	Pb 3,17	Th 0,20	U 0,33
Be 0,06	Sc 0,30	V 3,04	Cr 6,90	Co 0,69	Ni 7,55	Cu 49,60	Zn 39,15	Ga 0,47
Rb 5,15	Sr 405,83	Y 0,62	Zr 3,51	Nb 0,32	Mo 0,95	Cs 0,05	Ba 10,98	La 0,63

A sample of the dark brown, resinous wall coating applied unevenly to the upper areas of the Red Pyramid's inner chambers are presented here (at left), showing the specialized composition of trace elements that include strontium (Sr), copper (Cu), Zinc (Zn), barium (Ba), nickel (Ni) and rubidium (Rb). Iron oxides are predominantly present in the form of magnetite (Fe_3O_4), with a small component of red iron oxide (Fe_2O_3) and manganese oxide (MnO) powders, giving the material its dark brown coloration. As previously noted of the multi-ferrite geopolymer cement samples from the Central Pyramid, every one of the trace elements has been utilized in ferrite composites for modern electronic devices for diverse applications. The coatings must have been applied for generating magnetically-driven ferroelectricity and ionizing radiation within the resonant inner chambers of the Red Pyramid.

Several areas within passageways and corbeled chambers of the Red Pyramid present applications of the same orange multi-ferrite geopolymer cement (below) sampled and analyzed from water treatment systems surrounding the Causeway Temple of the Central Pyramid. Analytical electron microscopy results for this sample were not provided, but likely fall within the ranges for elemental composition seen in other samples.



Ferrite cement sampling site
Red Pyramid - Dashur, Egypt



Pulverized ferrite cement
Red Pyramid - Dashur, Egypt

The very same type of multi-ferrite geopolymer cements were applied to mosaic pavements cast in synthetic limestone in Edmond, Oklahoma. These magnetic, kaolin-based geopolymer cement coatings contain oxides of iron, nickel, titanium (brookite) and various other exotic particulate metals.¹³ Rumors have intimated these pavements at Edmond contain a small percentage of radioactive metal components, which is consistent with a strontium-barium ferrite composition (overleaf).¹⁴ The origin of these extensive pavements leads back to >29,000 bp, which can be determined by RC¹⁴ analysis of wood fragments embedded in the cement matrix.

The Atlantean mosaic floor in Edmond, Oklahoma (35.5946°N, 97.5062°W) is situated 6,824 miles from the Great Pyramid; corresponding to 27.41% of Earth's mean circumference. This resonant distance interval reflects the value of Fibonacci #154 ($6,833.00... \times 10^{-28}$) in miles, and the value of Fibonacci #377 ($27.46... \times 10^{-77}$) in percent, conforming the global mandala distribution pattern of the Atlantean pyramid network.



Mosaic pavement
Geopolymer limestone
Edmond, Oklahoma





Pavement tile, ferrite-coating
Geopolymer limestone
Edmond, Oklahoma



Large areas of ancient ferroelectric pavements were reburied and suppressed after their official dismissal as a natural geological feature. The temple platform is now situated below a strip mall and parking lot. Even if it were a natural feature, it would still be worth conserving and restoring for future museum display, being one among many ancient sites that are associated with underground cities hewn into the rock strata far below.

The same specialized multi-ferrite cement coatings have been painted onto magnetic geopolymer basalt pavements of the Parantha Pyramid Complex (below), located in the Blue Mountains of northeast Oregon and southeast Washington State.¹⁵ Their small dimensions and exotic ferrite composition confirm their origin as walkway pavements cast by gnomes of the Atlantean high civilization, applying the same chemical formulation that purposefully incorporates long-lived radionuclides for vitalizing the human body.



Ferrite-coated tiles
Parantha Pyramids

Time and again, archeological investigations at major ancient temples arrive at the inescapable conclusion that, despite their humble size, the exotic metallic composition of these pavement tiles is extraordinary, and closely matches that observed in the ISIDA Project chemical analyses of the Giza Plateau oxide samples.

What purpose to such radiations serve when used in potentially hazardous quantities? The answer to this fundamental question was actually addressed in general terms by the Nazarene One. The Essene Master Jesinavarah spoke directly of atomic decay radiations as the 'Fire of Life'. "Master, where is the fire of life?" asked some of them. "In you, in your blood, in your bodies."¹⁶ The limited terms available to Christ at the time of His teachings find transcendent meanings today, in the fundamental context of atomic physics:

For all the manifold gifts of Life, we do worship the Fire of Life, and the Holy Light of the Heavenly Order... The most beneficial and most helpful, the Fire of Life! The most supporting, the most bountiful, that Fire which is the House of the Lord!... A sanctuary of the Holy Spirit is the body in which the Fire of Life doth burn with eternal Light.¹⁷

High knowledge expressed by the Essene Master has mystified audiences since the moment these words were spoken, yet only find their fulfillment at the present time, with the revelations of quantum physics given at the time of the great transition of planet Earth and our human civilization to a high resonance domain. The vital forces of all living organisms are stimulated by the radiant cosmic and atomic forces of Nature, according to cascading decay reactions of the Earth itself –defined by the Heavenly Order of the elements.

Supremely advanced knowledge of quantum biophotonics demonstrated in such simple language in Judea was seeded for fruition in our present time, when higher development of the material sciences would outpace the growth of spiritual awareness. The bold statements of Christ preface the eventual rediscovery of the actual ET origin of humanity on Earth, *as a bioengineered Plejaren-Neanderthal hybrid species*.

Pavement tile, ferrite-coating
Magnetic geopolymer basalt
Parantha Pyramids, Washington



An exhaustive compendium of Atlantean votive names given throughout the course of the life's work of Edgar Cayce has been translated in previous work by this author¹⁸, based on the breakthrough epigraphic decipherment of K. Schildmann.¹⁹ These spiritual names aptly describe the internal *radiological* 'burning' of γ-ray exposure resulting from the purposeful ingestion of Atlantean Siddha bhasma pills, which induce painful burning sensations throughout the body when applied at high dosages for physical rejuvenation.

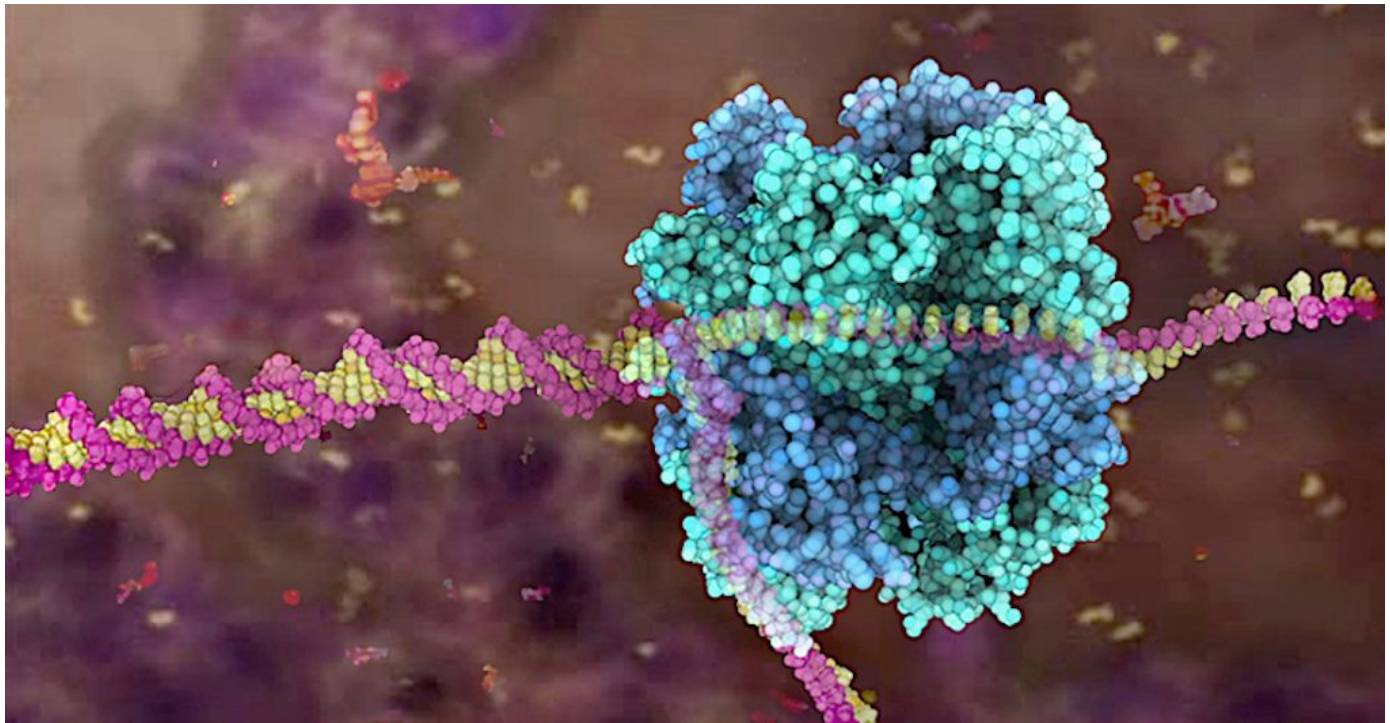
Name	Hieroglyphs	Meaning
Aidol	a id ol	"Ah, going aflame, burning"
Aidser	a id ser	"Ah, going aflame, binding"
Ajax-ol	aj ax ol	"Motive axis burning"
Apt-uldan	a pt ul dan	"Ah, arrival (of the) burning gift"
Ar-aptul	ar a pt ul	"Son, ah, (of the) arrival (of the) burning"
Arn-art-el	arn art el	"Bearing (the) pain (of the) Divine"
Arn-tini-n	arn ti nin	"Bearing (the) pervading essence"
Art-ex-elo	art ex el o	"Pain (of the) exceeding Divine, oh"
Artexi	art ex i	"Pain (of the) exceeding This"
Artshi	art s hi	"Pain from within sending forth"
Ast-elaart	ast el a art	"Casting (of the) Divine, ah, (the) pain"
Astu-bed	as tu bed	"For conferring activation"
Atlant	at lan t	"Pervading luminosity (of) protection"
Atlanteus	at lan te us	"Pervading luminosity (of) Their dawning"
Atlantis	at lan tis	"Pervading luminous radiance"
Aulda	a ul da	"Ah, (the) burning giving"
Bel-elduen	bel el du en	"Activating (of the) Divine, being burnt (by) That"
Belial	bel i al	"Activating (of) This, (of the) ability"
Betha-old	be th a ol d	"Activity (of the) unutterable, ah, (the) burning unending"
Denuol	d en u ol	"Endless That, oh, (the) burning"
Dieol	di e ol	"Desirous submission (to the) burning"
Du-denlu	du d en lu	"Being burnt (by) the endless, That allure"
Dul-extop	d ul ex t op	"Endless burning (of the) beyond, protection meeting"
Du-lo	du lo	"Being burnt, lo"
Duo-she-dui	du o she du i	"Being burnt, oh, splendor (of) being burnt (by) This"
Edu-on	e du on	"Submission (to) being burnt (by) assent"
Poseida	pos e id a	"Reverberating submission (to) going aflame, ah"
Shu-artso	shu art s o	"Cleanly pain from within, oh"
Shu-gun-gin	shu g un g in	"Cleanly spark, (the) uplifting spark (of) glory"
Su-enphti	su en ph ti	"(The) good (of) That manifesting rays"
Su-gahdt	su g a hd t	"(The) good spark, ah, with (the) progeny (of) protection"
Susuśus	su s us us	"(The) good from within, dawning punishment"
Tul-mep-on	t ul me p on	"Protection (of the) burning, bleating inner joy (of) assent"
Ulda	ul da	"(The) burning giving"
Ulhñ	ul h ñ	"(The) burning (of the) imperceptible presence"
Ultzer	ul t ze r	"(The) burning protection (of) serving (the) turning"
Undui	un du i	"(The) uplifting (of) being burnt (by) This"
Usdus-tan	us du s t an	"Punishment (of) being burnt from within; protection (of the) Breath"
Vedus	ve du s	"Knowing (of) being burnt from within"

Such explicit names such as "*Knowing of being burnt from within*" by the "*burning gift*" present unmistakable references to the attainment of high knowledge pertaining to *radiological burning experienced within the body*—exalting the very same life-giving atomic forces praised by the Essene Master in much more recent times. The specific wording of sacred names given by the Atlantean psychoacoustic society was especially relevant because they were given to newborn infants procreated by conception and waterbirthing practices within the red granite resonator box of the Great Pyramid, in the highest focal point of planetary infrasound.

'Flying Siddha' Bokar made unequivocal statements inviting his pupils to ingest radium-containing Brammam bhasma for illumination within: "Light yourself on fire!" Unfortunately, this traditional Siddha metaphor has been taken out of its proper context by Buddhist monks who turn to self-immolation as a means of protest.

How is it that potentially lethal radiation sources such as the Ark of the Covenant were manufactured and used in sacred ritual activities by various cultures in ancient times? Such counter-intuitive ethnographical and archeological evidence can only be understood by examining the broader biological context of DNA damage repair mechanisms that become differentially engaged under the influences of various radiations.

The latest research quantifies destructive effects on the DNA double helix wrought by ionizing radiation of all kinds, which can be divided into 2 groups by intensity of energy deposition. X-ray, γ -ray and electron radiations are sparsely ionizing, in contrast to the intensely ionizing effects of heavy ion, α -particle, proton and neutron radiations. Absorbed doses of ionizing radiation are calculated according to their effects:



The radiation exposure is equivalent to the energy "deposited" in a kilogram of a substance by the radiation. Exposure is also referred to as absorbed dose. The important concept is that exposure is measured by what radiation does to substances, not anything particular about the radiation itself. This allows us to unify the measurement of different types of radiation (i.e., particles and wave) by measuring what they do to materials.²⁰

Exposure levels for ionizing radiation received from both particulate and waveform emissions are measured using a large unit, the gray (Gy), and its various subunits defined according to the following specifications:

1 nanogray (nGy)	=	0.000000001 Gy (1/1,000,000,000)
1 microgray (μ Gy)	=	0.000001 Gy (1/1,000,000)
1 milligray (mGy)	=	0.001 Gy (1/1,000)
1 centigray (cGy)	=	0.01 Gy (1/100)

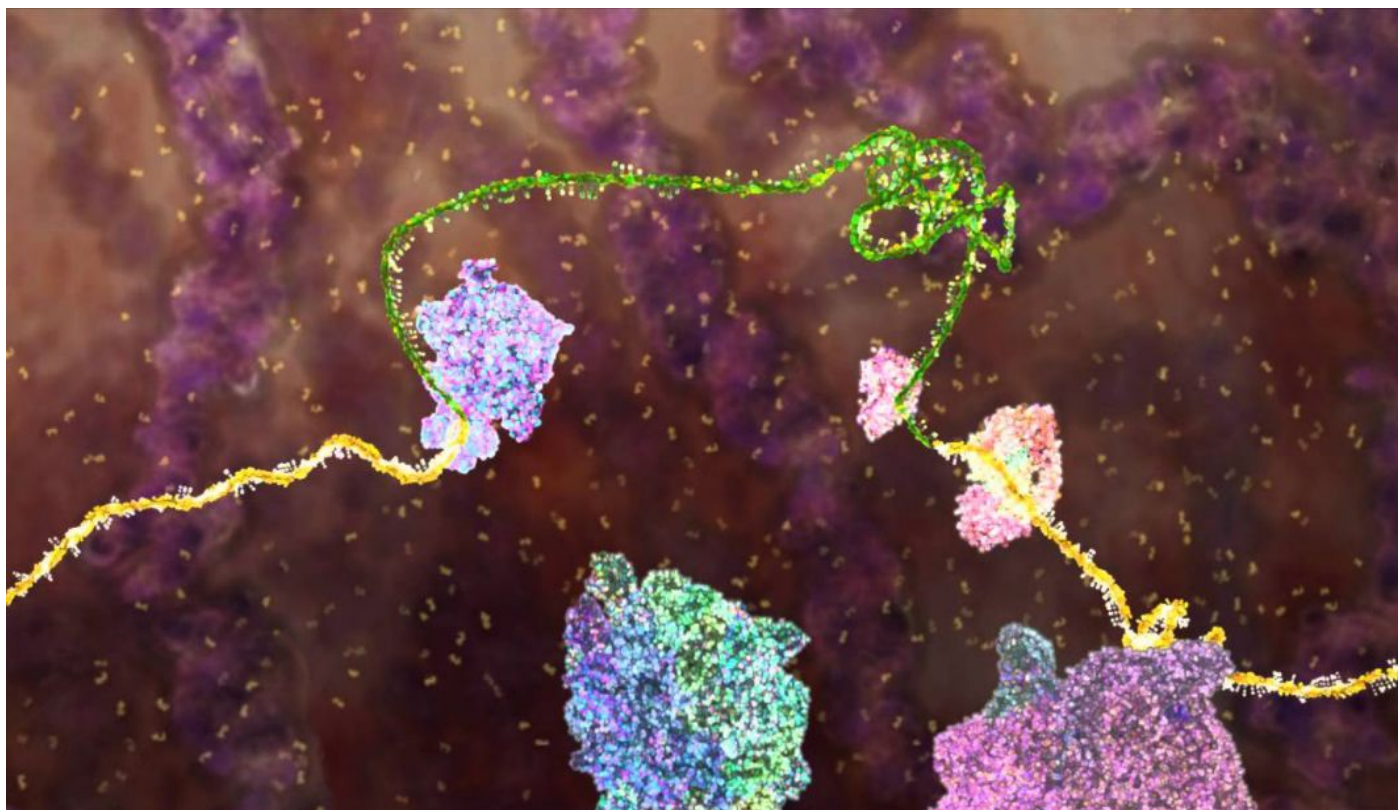
Other units are also used in the measurement of radiation levels, including the Sievert (Sv) and Roentgen (R) and their respective subunits. A general comparison of relative levels of full body exposure is given here, based on scientific data for γ -radiation exposure compiled over recent decades from various sources:

- Average background radiation dose for cosmic radiation received outdoors at sea level: 30 nGy/h
- Low-dose / low dose rate for γ -radiation: 0.04 Gy (40 mGy) @ 2.2 mGy/hr total body exposure
- Intermediate-dose / intermediate dose rate for γ -radiation: 0.4 Gy (40 cGy) @ 2.2 cGy/hr total body exposure
- High-dose / high dose rate for γ -radiation: 2 Gy @ 0.425 Gy/hr total body exposure
- Total body exposure to 4 Gy @ 0.425 Gy/hr causes sickness and death in half of exposed individuals
- Total body exposure to >10 Gy @ 0.425 Gy/hr causes sickness and death in all exposed individuals in 3-10 days
- Rapid-acting, lethal dose and acute dose rate for γ -radiation: >20 Gy @ 1 Gy/min causes death in >20 minutes

A 2004 study identified the comprehensive benefits of full body exposure to single micro-doses of low-LET ionizing radiation, effectively initiating an *adaptive protection response*. Beneficial effects are reported to last from several hours to several weeks, including enhancement of cell signaling and apoptosis, stimulation of the free radical detoxification system, reduced incorporation of DNA precursors and of thymidine kinase activity, elevated levels of glutathione and superoxide dismutase, as well as decreased lipid peroxidation.

The adaptive protection response observed after IR exposure has been linked with dynamic changes in gene expression. Altered expression of more than 100 genes, including telangiectasia and other stress response genes, was observed within 2 hr of IR exposure. This adaptive protection response in mammalian cells was maximized at exposures of 5-200 mGy, with diminishing effects observed with increased dosage.²¹

Contrary to false assumptions perpetuated by government-funded scientists for the last century, exposure to low dose γ -radiation enhances the DNA damage response regime applied by the cells of the body. The general parameters influencing DNA repair mode expression indicate optimized states promote homologous repair mechanisms requiring enhanced cellular metabolism to maintain high-fidelity DNA restoration.



For this specific reason –to significantly increase energy production of mitochondria in cells throughout the body– traditional Siddha and Ayurveda medicine applies photoluminous herbal and mineral nanopowder combinations in pill form for ingestion. In allopathic medicine, the practice of eliciting beneficial effects from micro-doses of potent toxins is called '*hormesis*'; an art form that is applied masterfully by Siddha adepts who directly inherited the sacred gift of ancient alchemical knowledge from the high civilization of Atlantis.

Ancient Atlantean temple traditions also applied advanced phonon transfer alchemy methods for generating colloidal elixir waters, extolled as Soma; beverage of the gods. Soma preparation transmutes surfaces of silver nanoparticles into technetium (Tc^{96}) for emitting β^+ decay products (electron neutrinos) and aqueous osmium tetroxide (OsO_4) gas. For this reason, every phonon drinking vessel was called a 'Chalice of Life'.²²

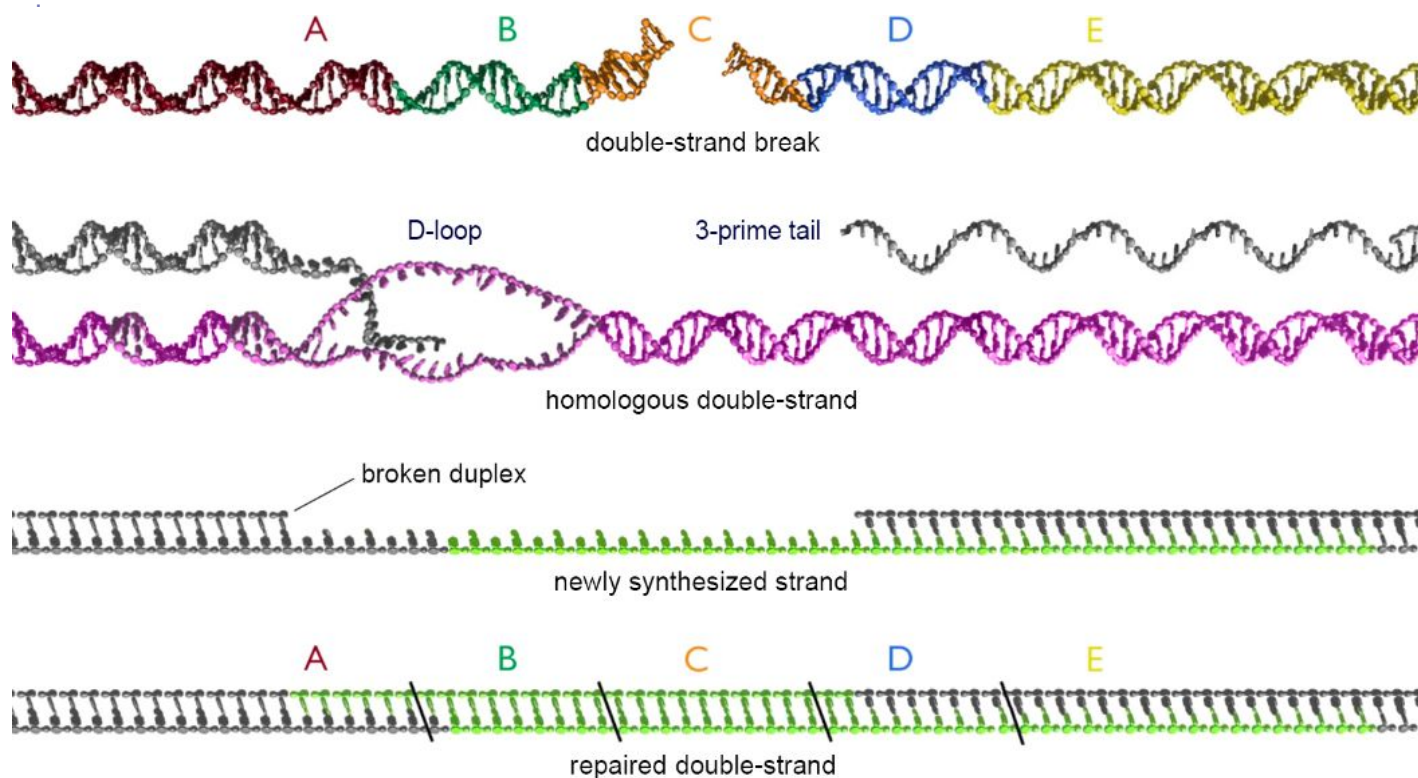
Neutrinos enhance psychic reception, whereas osmium tetroxide gas is a potent superoxide dismutase that dissolves dead tissue within the various tracts of the body, complimenting the production of endogenous superoxide dismutase by the body's cells as an adaptive response to ionizing radiation exposures.

The specialized biophotonic function of rasayana bhasma elixirs often prescribed by Siddha and Ayurveda practitioners went entirely unrecognized until the present work of this author, which provides the only viable explanation for the extreme longevity of Siddha saints –documented in several cases to exceed 250 years. Biophotonic activation of high metabolism by the interaction of bhasmas engages the most efficient DNA repair process for restoring double-strand breaks in the helix, called *homologous recombination* (HR):

The DNA helix is broken by a double-strand break in the C region. To begin the repair process, double-strand breaks in the DNA first undergo nuclease degradation, to yield duplexes with 3-prime-ended single-stranded tails. These tails may be hundreds of base pairs long.

In a process mediated by recombination proteins, one of the single-stranded 3-prime-ended tails from the broken parental duplex (shown in grey) interacts with the homologous duplex (shown in pink), such that the grey single strand invades the pink duplex at a region of homology...

This loop structure, together with the invading strand, is called a displacement loop or D-loop. The 3-prime end of the invading strand then acts as a primer for DNA synthesis... [as] a small bubble containing the template, a short region of the newly synthesized DNA and the displaced strand forms and tracks across the pink template strand..



The replication bubble dissociates and the newly synthesized strand (shown here in green) is then captured by the 3-prime-ended single-stranded tail from the other side of the break in the duplex... The newly captured 3-prime hydroxy end of the broken duplex then serves as a primer for new DNA replication across the break, and extending to the other side of the break. Remaining gaps are then filled by replication and ligation. Note that, overall, the gap in the double-strand break where the degradation occurred (the C region) has been repaired by new DNA synthesis; the template for which was a duplex homologous to the broken DNA.²³

This high-fidelity, homology-dependent DNA damage repair process only becomes engaged under specific conditions, and only when the required energy resources are available to each cell to sustain its heightened activity. Many lines of archeological evidence reveal Atlantean temple stones, funerary items and spacecraft metals promote restorative DNA repair via full body exposure to γ -radiation from long-lived radio-isotopes.

The specialized biophotonic functions of the pyramids optimize the activation of DNA damage responses that were only recently modeled by modern genomic scientists in 2022. The highly complex and counter-intuitive engagement of DNA damage repair processes *becomes optimized under exposure to low dose γ -radiation*:

Charged-particle radiotherapy (CPRT) utilizing low and high linear energy transfer (low-/high-LET) ionizing radiation (IR) is a promising cancer treatment modality having unique physical energy deposition properties... Further improvements in CPRT are expected from a better understanding of the mechanisms governing the biological effects of IR and their dependence on LET. There is increasing evidence that high-LET IR induces more complex and even clustered DNA double-strand breaks (DSBs) that are extremely consequential to cellular homeostasis, and which represent a considerable threat to genomic integrity...

Sparsely ionizing x-rays
DNA damage response



Here, we review the specific cellular DNA damage responses (DDR) elicited by high-LET IR and compare them to those of low-LET IR. We emphasize differences in the forms of DSBs induced and their impact on DDR. Moreover, we analyze how the distinct initial forms of DSBs modulate the interplay between DSB repair pathways through the activation of DNA end resection. We postulate that at complex DSBs and DSB clusters, increased DNA end resection orchestrates an increased engagement of resection-dependent repair pathways...

Reports dating as far back as 1902–1904 corroborate the application of radium in treating neck carcinomas and delivering radiation through glass tubes placed in close proximity to the tumors—a precursor of interstitial brachytherapy. At present, photon beam radiotherapy in the form of low-LET X-rays is the standard and most widely used treatment in clinical settings worldwide...

It is well-established that low-LET IR modalities, such as γ -rays or X-rays, generate various forms of DNA lesions through either direct ejection of an electron from the DNA, or attack by a hydroxyl radical ($\cdot\text{OH}$) produced by the radiolysis of water. The wide spectrum of generated DNA lesions includes sugar and base damages, as well as DSBs that are induced at ratios of about 20:1. Some forms of sugar damage disrupt the phosphodiester backbone of the DNA molecule and produce single-strand breaks (SSBs)...

When ionization clusters hit the DNA, they can evoke damage on both strands of the double helix and, thus, give rise to DSBs. The prevailing assumption in the field is that the adverse biological effects of X-rays or γ -rays derive from DSBs generated within such ionization clusters, rather than by independently generated ionizations on opposite DNA strands. Despite the generation of ionization clusters at the ends of low energy electron tracks, X-rays and γ -rays still deposit 50-70% of their energy in distinct ionization events. The latter derive from high-energy electrons that ionize sparsely and generate a relatively even ionization pattern within the cell. This is why X-rays and γ -rays are considered sparsely ionizing forms of IR (Figure 1).

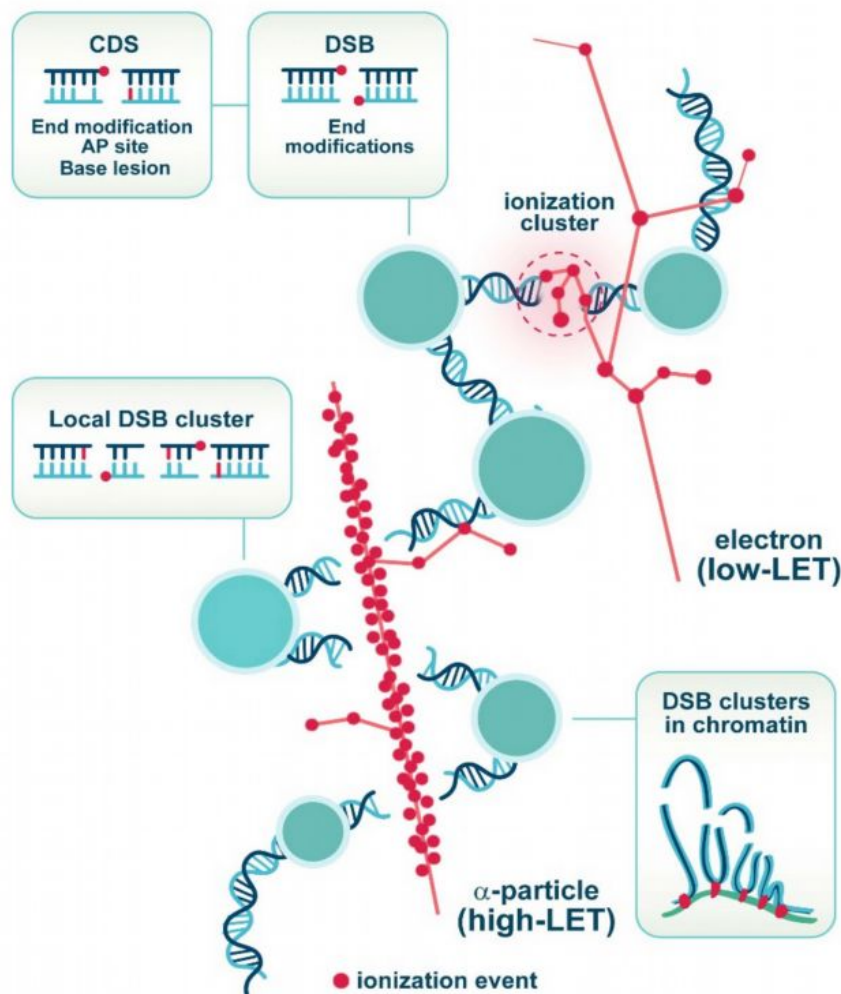


Figure 1. Generation of DSBs by low-LET electrons and high-LET α -particles. Ionization events along the radiation tracks are presented as red dots, while the DNA molecule is rendered as part of chromatin organized with nucleosomes. The formation of DSBs of different complexity is induced by both low- and high-LET IR and these DSBs frequently harbor chemically modified DNA ends that are not directly ligatable and require additional processing. Clustered damage sites (CDS) of different damage permutations are detectable after low-LET IR and their number increases with increasing LET. Notably, high-LET IR generates with significantly higher probability DSB clusters, comprising multiple DSBs located in close proximity along the DNA that destabilize chromatin and, thus, the processing of the individual DSBs that always takes place in the context of chromatin...

There are also distinct biological advantages associated with the use of heavy ions (HI). Enhanced ionization clustering generated by high-LET particles, as compared to secondary electrons produced by low-LET X-rays, correlates with increased complexity/clustering of the damage induced in the DNA. Complex damage comprises at least two DNA lesions within one helical turn of DNA...

The production of short DNA fragments with increasing LET has also been associated with increased cellular toxicity and lethality. The latter is attributed to the impaired bilateral binding of KU70/80-heterodimer, a key component of classical non-homologous end-joining (c-NHEJ), on such very short fragments. In line with these findings, it has also been shown that short DNA fragments (14–20 bp) impede the activity of the DNA-PK holoenzyme. In aggregate, available results suggest that high-LET IR compromises the efficiency of c-NHEJ, which causes a switch towards resection-dependent DSB repair pathways...

The results presented in this report confirm that increased DSB clustering correlates with increased cell lethality... High-LET IR produces clearly higher DSB yields than low-LET X-rays, with up to ~500 DSBs per μm^3 track volume. A substantial fraction of these heterochromatic DSBs persist for longer periods of time suggesting difficulties in their repair. By contrast, DSBs induced by low-LET IR are efficiently rejoined within 24 h, both in eu- and heterochromatin. These data in aggregate support the hypothesis that the spacing and quantity of DSBs in clustered lesions affect DNA repair efficiency, and may determine the radiobiological outcomes...

A key target of DDR signaling is the regulation of DSB repair that is essential for the restoration of DNA sequence and structure to safeguard genome stability. Higher eukaryotes have evolved 4 major DSB repair pathways, which have distinct cell cycle and DNA sequence homology dependencies and operate with diverse fidelity and kinetics. Classical Non-Homologous End Joining (c-NHEJ) is the predominant DSB repair pathway. It operates throughout the cell cycle without requirements for homology, although it occasionally utilizes microhomologies of 1–4 bp.

Homologous recombination (HR) exhibits pronounced cell cycle dependence and operates only in S and G₂-phase of the cell cycle when a sister chromatid becomes available after DNA replication. HR requires long stretches of homology –typically more than 100 bp. Alternative end-joining (alt-EJ) typically requires microhomology of at least 2 bp (usually more) and <20 bp. Single-strand annealing (SSA) requires longer tracts of homology than alt-EJ that may occur on the same DNA molecule. A major discriminating characteristic between c-NHEJ and all remaining DSB repair pathways is its independence of resection at DSB ends. As a consequence, DSB repair pathways are frequently classified as resection dependent (HR, alt-EJ and SSA) and resection independent (c-NHEJ)...

IR modalities of different LET elicit distinct biological effects reflecting changes in DSB character and processing. However, what causes these changes? High-LET IR induces highly complex, as well as clustered DSBs that compromise the prevailing hierarchy in DSB repair programs and generate a shift from resection-independent c-NHEJ towards resection-dependent repair mechanisms. This is a clear adaptation cells make to necessities generated by the type of DSBs induced, and which dictate their processing. It manifests with the engagement of lower fidelity repair pathways, presumably because of their lower overall operational requirements for chromatin stability, and their ability to deal with DNA ends that have drifted away from each other for several reasons, including the severity and extent of breakage.

A plausible model of DSB repair pathway engagement integrating known biological responses to low- and high-LET IR for cells irradiated in G₂-phase (selected because all DSB repair pathways are active) is shown in Figure 4. According to this model, when cells are exposed to low doses of low-LET IR, c-NHEJ and HR contribute almost equally to DSB repair. The shift at low doses to error-free HR allows restoration of the genome with maximum fidelity. Mutagenic DSB repair processes including c-NHEJ, alt-EJ and SSA are partly or completely suppressed and only operate when HR fails to engage or complete. With increasing IR-dose of low-LET IR, HR is suppressed by mechanisms that remain to be characterized, while c-NHEJ clearly gains ground and becomes first choice. DNA end resection also remains active showing signs of suppression only above 20 Gy. Persisting resection under conditions of suppressed HR leads to increased engagement of error-prone alt-EJ and SSA:

DSB Processing and Repair for Cells Irradiated in G₂-Phase

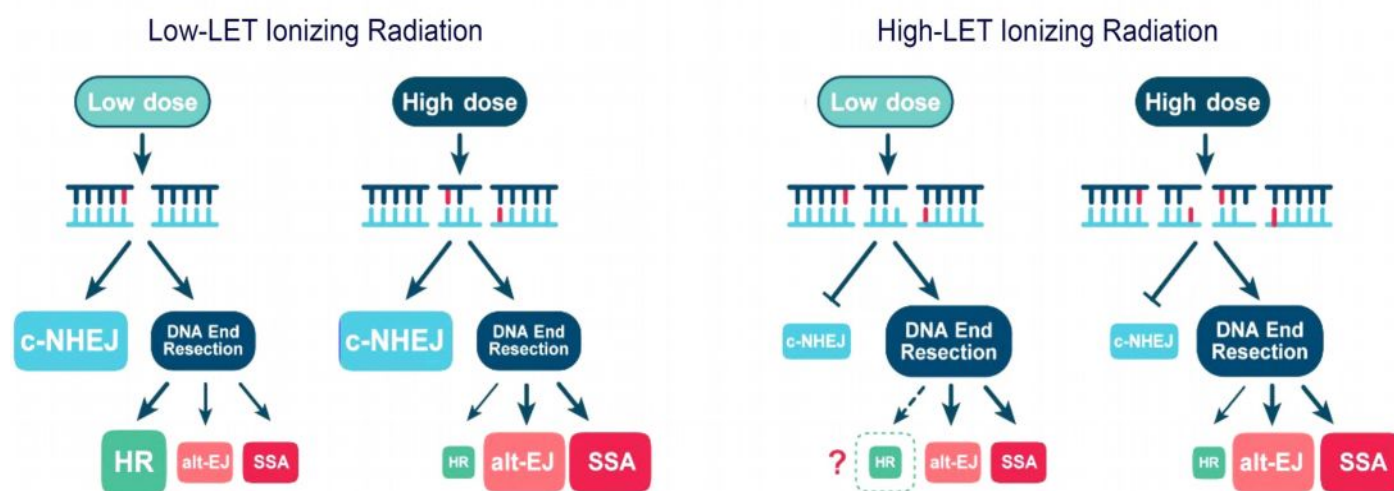


Figure 4. Exposure of cells to high-LET IR disrupts the balance between DSB repair pathways by shifting the processing to DNA end resection-dependent mechanisms

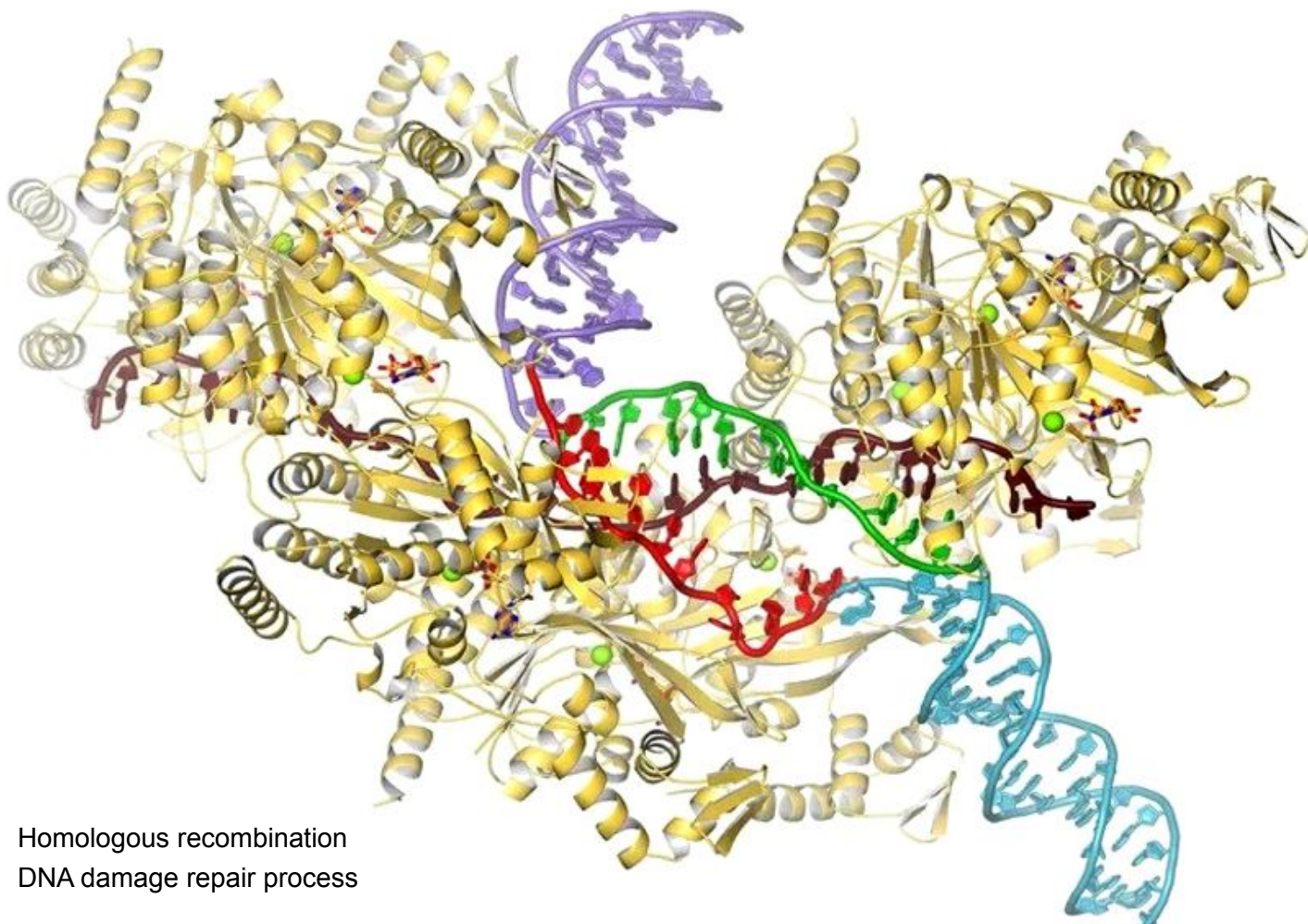
On the other hand, when complex DSBs or DSB clusters are generated by exposing cells to high-LET IR, several profound changes in repair pathway balance take place. Perhaps the most profound is the suppression of c-NHEJ (at least for the subset of DSBs that determine cell survival)...²⁴

These important findings reveal the effects of varying types and intensities of radiological exposures on the differential engagement of DNA damage response pathways in eukaryotic cells: “With increasing... dose of low-LET IR, HR is suppressed by mechanisms that remain to be characterized, while c-NHEJ... becomes first choice... On the other hand,... exposing cells to high-LET IR [induces]... the suppression of c-NHEJ.”

Rejuvenatory rasayana elixirs of the Siddha yogis of ancient India implicate low cellular metabolism as the root cause of the suppression of the HR repair pathway, which requires increased energy resources from mitochondria. Ingestion of bhasma pills composed of nanopowdered herbs and photoluminescent sulfides –including radium sulfide– applies red photon emissions for stimulation of mitochondria, thereby promoting high-fidelity processing of complex DSBs by preferential engagement of the superior HR repair mode.

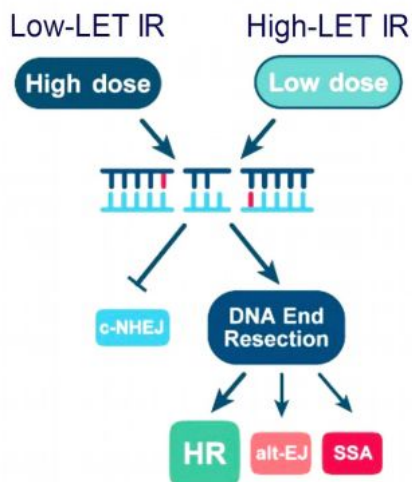
Further investigations of the biological effects of exposure to ionizing radiation from dual sources will confirm the efficacy of Siddha regenerative medicine, which masterfully applies natural radiation from the long-lived, non-toxic α -decay source called *Brammam* in Sanskrit; and known today as radium (Ra²²⁶).

High knowledge of these biological responses was applied by ancient Atlantean temple practitioners for simultaneous activation of the qi meridian system by ingesting the same bhasma pill formulations used by Siddha adepts thousands of years after the demise of Atlantis. Excited by γ -radiation from radium sulfide (RaS) nanoparticles, red photon emissions enhance metabolic activity in mitochondria whereas sterilizing UV-B and -C photons are prescribed for reducing microbial pathogens throughout the body.²⁵



Homologous recombination
DNA damage repair process

Radiological Longevity Among Cigar Smokers, Siddhas & ETs



Cigar smokers (110+ yrs)
 Po^{210} (0.379 y)

Siddha adepts (300+ yrs)
 Ra^{226} (1,600 y)

ET visitors (1000+ yrs)
 Mc^{296} (>500,000 y)

These results indicate DNA repair is not optimized by applying low-dose ionizing radiation, but by ingestion of natural α -decay emitters at specific doses. Lung tissue exposure among heavy cigar smokers to Po^{210} α -decay emissions extends average lifespans to 110+ yrs.²⁶ Extreme longevity of 300+ yrs are achieved by Siddha adepts by applying Ra^{226} , while ET visitors enjoy average lifespans of 1000+ yrs by applying synthetic Mc^{296} . Long-lived α -emitter isotopes provide optimal proportions of high-dose low-LET γ -radiation and low-dose high-LET α -particles –*blocking c-NHEJ mode while promoting HR repair*.

In contrast to the case of heavy cigar smokers, cigarette smokers do not receive comparable benefits in longevity due to the poisonous effects of carcinogenic ‘burning agents’ that have been purposely added to the ancient herbal remedy by tobacco companies to hide its great efficacy in cancer prevention. The same is true in the case of cannabis smoke,²⁷ which delivers low doses of γ -radiation from Po^{210} in lung tissues.

An overwhelming abundance of evidence, gathered at Paleo-Sanskrit construction sites located on every continent, demonstrates that ancient builders of the Atlantean Era produced artificial temple stones loaded with radionuclides. The vitalizing biophotonic emissions of Siddha bhasma preparations are activated by Ra^{226} , whereas Atlantean elixirs from the first phase were activated by superheavy isotope Mc^{296} , reflecting high knowledge concerning phonon transmutation of synthetic moscovium and technetium (Tc^{97}) isotopes.



Accurate assessment of the optimal status of DNA damage responses explains sacred vitalizing functions of the Ark of the Covenant (illustrated above), exhibiting potent radiological effects of a gold-based alloy containing $>5\%$ metastable superheavy isotope Mc^{296} . Ron Wyatt (†1933-1999) died of cancer induced by prolonged exposure to high-intensity radiations from the Ark of the Covenant, stored in ‘Jeremiah’s Grotto’ below the Calvary Hill crucifixion site under the full-time monitoring and protection of ET ‘guardian angels’.

Similarly high levels of superheavy Mc^{296} content are implicated in the case of the Baigong Cave pipes at Toson Lake, China. A careful metallurgical investigation is warranted for identification of superheavy isotopic content, which was reported as an ‘unknown metal’ at the time of the initial spectroscopy study in 2007.²⁸ Thermoluminescence dating results place the origin of the Baigong Cave site to $\sim 150,000$ years,²⁹ placing it directly before the timeframe of $\sim 107,000$ bp given by Edgar Cayce for the origin of modern humans.

Similar types of geopolymer sandstones ferrites loaded with exotic elements found at Heavener Runestone State Park, Oklahoma also represent radioactive pavements dating to an early phase of Atlantean civilization (overleaf).³⁰ Geometric bands of hard metallic sandstone are interspersed with softer bands with less metals.



Ferrite sandstone walkways
Heavener, Oklahoma

Ferrite sandstone walkways
Shaw Beach, West Virginia





Ferrite sandstone walkways
Shaw Beach, West Virginia



Heavener Runestone State Park, Oklahoma (34.898206°N, 94.5781216°W) is located 6,743 miles from the Great Pyramid of present-day Giza, Egypt, representing 27.09% of Earth's mean circumference distance. These geopolymer sandstones present distinctive red seam-work that has hardened by the migration of iron oxides and other trace metals from an initial coating applied to the interior of each mold before casting. The sandstone pavements' iron features are characteristic of the third phase of Atlantis, from 30,000-13,000 bp.

Nicknamed 'Waffle Rock', a large, geometrically-tiled sandstone platform was discovered at Shaw Beach, West Virginia (39.428801°N, 79.1238335°W, opposite, overleaf). Sections were removed from the original platform for domestic displays, having been erroneously identified as a rare geological feature (below).

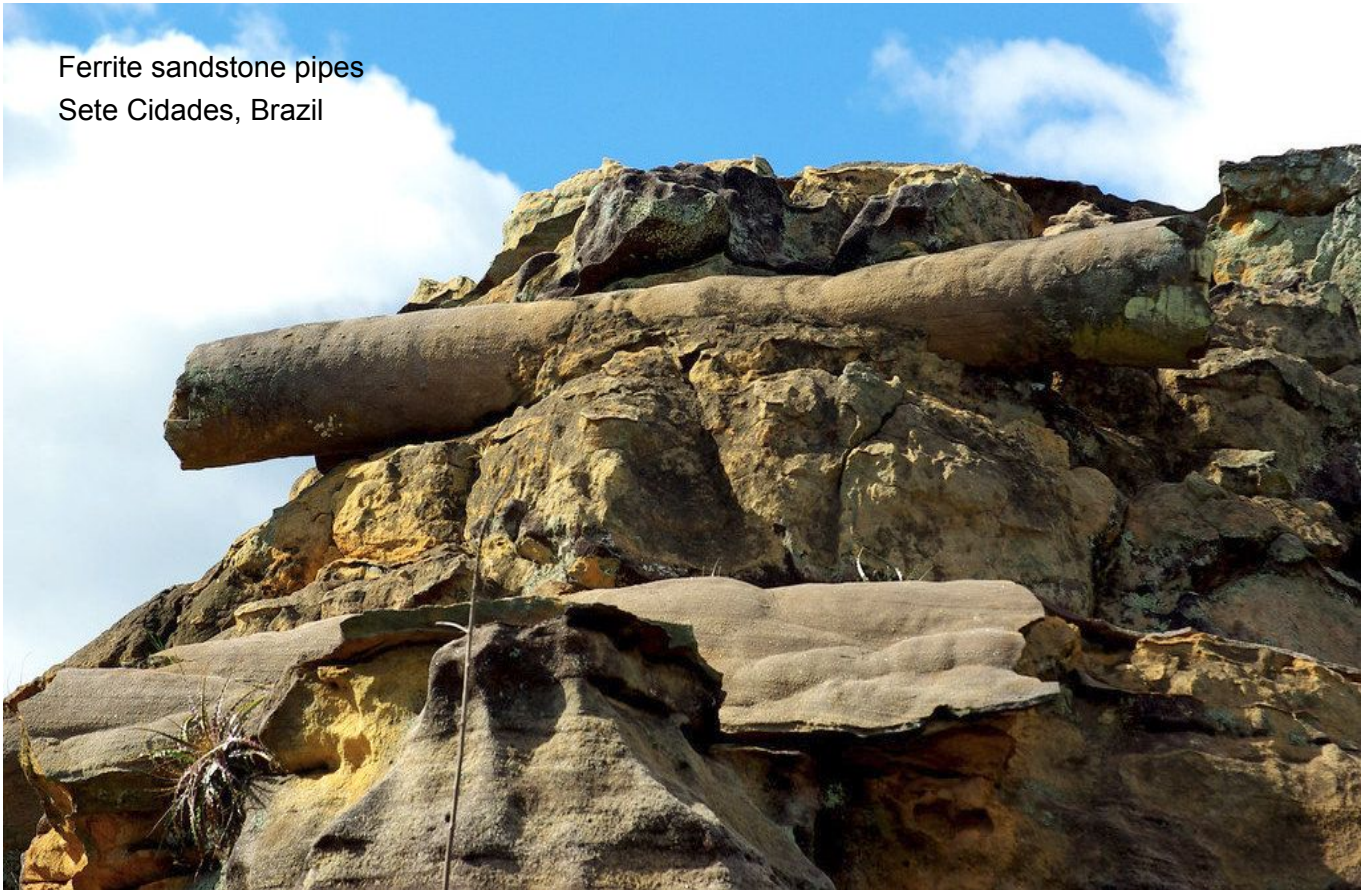


These geometric configurations present grid-work composed of sets or parallel lines that form rhombohedral and triangular cells, with the softer sandstone in the center of each tile worn away to leave the raised edge-work. Iron-loaded sandstone geopolymer tile mosaics of this type were also found at Tea Creek Mountain, West Virginia (38.3337585°N, 80.1990037°W) and in Reston, Virginia (38.9441344°N, 77.3510258°W).

Synthetic stonework at these sites requires sampling for comprehensive chemical analyses and metering for sources of ionizing radiation to determine the potential radionuclide content of trace metal constituents. Metallic geopolymers were cast by hand during the third phase of Atlantis, which is easily discerned from stonework melted by HHO plasma beams during the first phase that extends back over 100,000 years.

Sete Cidades, Brazil (4.0968246°S, 41.6847978°W) is located 3,269 miles from the sunken Atlant Pyramid (29.9792458°N, 76.125°W), submerged off Florida. In addition to geopositioning near 4° South latitude, this resonant distance interval represents 13.13% of Earth's mean circumference, reflecting the value of Fibonacci #363 ($3,258.58... \times 10^{-72}$) in miles, and the value of Fibonacci #141 ($13.11... \times 10^{-28}$) in percent.

Ferrite sandstone pipes
Sete Cidades, Brazil





Ferrite sandstone pipes
Sete Cidades, Brazil



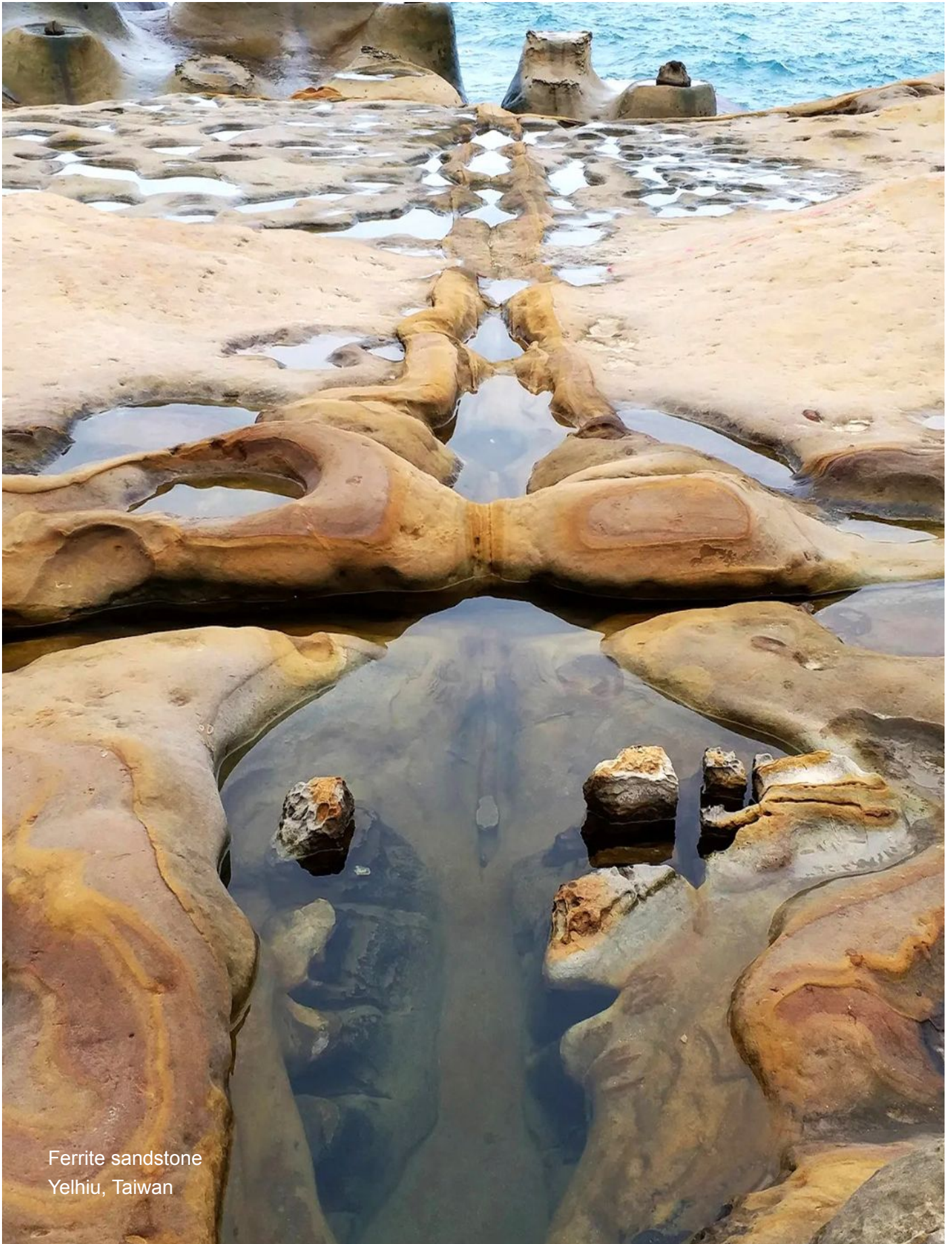
Ferrite mudstone pipes
Baigong Cave, Lake Toson
Qinghai, China



Close examination of the fragmentary remnants of ferrite sandstone pipe formations at Sete Cidades, Brazil shows many unmistakable similarities with the Baigong Cave pipes at Lake Toson in Quinghai, China (above). An investigation of the chemical composition of samples obtained from the Sete Cidades metallic geopolymer pipes will likely parallel those spectacular findings made by Chinese metallurgists in 2007.

These specialized features are the remnants of highly advanced water purification systems leading from the surface downward, reaching far below ground to provide filtration and exposure to high-intensity ionizing radiation for sterilization. Enhanced electrical conductivity is generated by piezoelectric transduction of the mudstone and sandstone geology of the site, *stripping nanoparticles of moscovium to form elixir springs*.

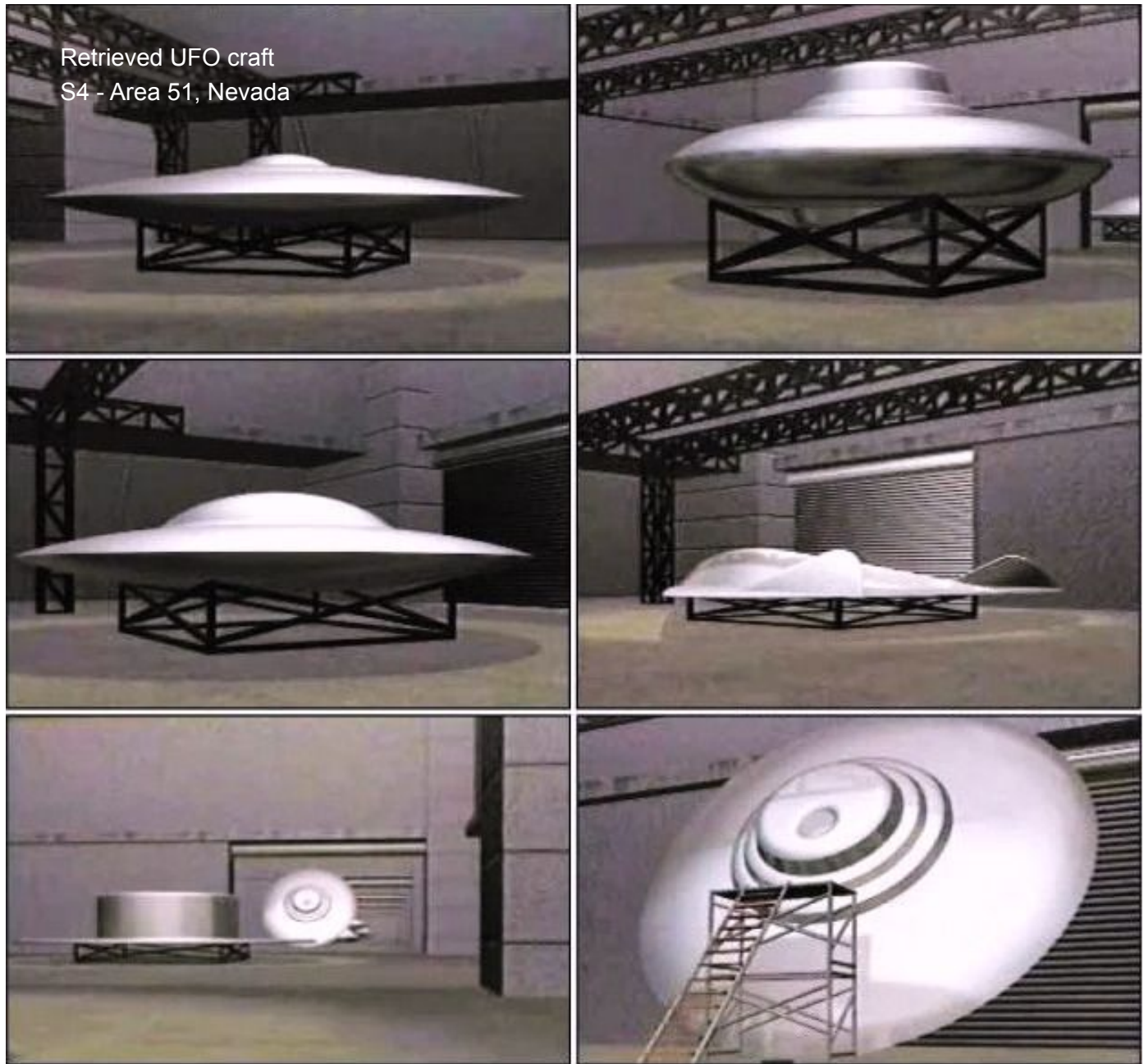
Such elevated technological achievements were accomplished by the Atlantean spiritual leadership of the Sons of the Law of One, through whom the access to high knowledge was shared worldwide, according to technology sharing accords that included manufacturing processes for antigravitic aerospace applications.



Ferrite sandstone
Yelhiu, Taiwan



Ferrite sandstone
Yelhiu, Taiwan



Aerospace vehicles of the same class have been obtained by covert UFO crash retrieval programs of the US military and related clandestine subcontractors. The hyper-compartmentalization of these projects in private corporations has significantly limited success in retro-engineering these vehicles. Advanced interstellar spacecraft are specifically designed for beings with a far superior biophotonic metabolism that is maintained by high-energy radiations within the craft –which are integral to its functioning.

For this reason, *terrestrial human beings of Earth cannot be in proximity to the craft for more than 15 minutes without receiving lethal radiation doses.* Many lives have been lost over the past 8 decades due to severe radiation exposure from the huge hulls and interior compartments of interstellar spacecraft.

Indeed, the same potential biohazard is presented by all ancient Atlantean pyramid cities, which were paved with geopolymer stone walkways painted in radioactive coatings. Spending full days or weeks on the Giza Plateau, in the Great Pyramid or in the underground palaces of the Great Labyrinth³¹ can also have lethal ramifications,³² for they all apply the same technological features as the Ark of the Covenant and recovered ET spacecraft. *High-radiation zones can only be utilized by ingestion of rasayana elixirs.*

References

- 1 -- (2023) 'Analyzing the North Face Corridor of the Great Pyramid' *Youtube*, online
· <https://youtu.be/AAxelvcgH1g>
- 2-- (2023) 'Episode 75: Chemical Analysis of the Giza Plateau Iron Oxide Deposits' *Youtube*, online
· <https://youtu.be/aP-oFvS9X-0>
- 3 Putney A (2009) 'Veil of Invisibility - A Selection from Chapter 1: Curious George' *Human Resonance*, online
· <http://www.human-resonance.org/george.html>
- 4 Hancock G (1995) '*Fingerprints of the Gods: The Evidence of Earth's Lost Civilization*' Crown, London
- 5 Putney A (2022) 'Metamaterials of Ajax' *Human Resonance*, online
· http://www.human-resonance.org/Metamaterials_of_Ajax.pdf
- 6 -- (2023) 'The ISIDA Project' *ISIDA Project*, online · <https://isida-project.org>
- 7 -- (2022) 'Episode 62: Major Discoveries Inside the Central Pyramid' *Youtube*, @16:50 online
· <https://youtu.be/XyvkHku0Pc4>
- 8 Lin J, Svensson A, Hvidberg CS, Lohmann J, Kristiansen S, Dahl-Jensen D, Steffensen JP, Rasmussen SO, Cook E, Kjaer HA, Vinther BM, Fischer H, Stocker T, Sigl M, Bigler M, Severi M, Traversi R, Mulvaney R (2022) 'Magnitude, Frequency and Climate Forcing of Global Volcanism During the Last Glacial Period as Seen in Greenland and Antarctic Ice Cores (60-9ka)' *Clim. Past* 18, pp. 485-506
· <https://cp.copernicus.org/articles/18/485/2022/cp-18-485-2022.pdf>
- 9 Baba PD (1965) 'Nonmagnetic Inclusions in Ferrites for High-Speed Switching' *J Am Cer Soc* 48(6), pp. 305-309
- 10 Mahmoud K, Makled M (2012) 'Infrared Spectroscopy and Thermal Stability Studies of Natural Rubber-Barium Ferrite Composites' *Adv Chem Eng & Sci* 2, online
· https://www.scirp.org/pdf/ACES20120300003_26470005.pdf
- 11 -- (2020) 'Hidden Chambers Filled with Sand - Great Pyramid of Egypt Facts...' *Youtube*, online
· <https://youtu.be/notz0z53wtM>
- 12 -- (2023) 'Episode 65: 2022 Osiris Shaft Documentary and Chemical Analysis' *Youtube*, online
· <https://youtu.be/Z-2zs4ajNm4>
- 13 Putney A (2018) 'Magnetic Pavements' *Human Resonance*, online
· http://www.human-resonance.org/Magnetic_Pavements.pdf
- 14 -- (2023) '200,000-Yr-Old Tiled Floor Found in Oklahoma?' *Youtube*, online · <https://youtu.be/PAX68qh0jVA>
- 15 Putney A (2019) 'The Parantha Pyramids' *Human Resonance*, online
· http://www.human-resonance.org/Parantha_Pyramids.pdf
- 16 Szekely EB Tr. (2018) '*The Essene Gospel of Peace - Books 1-4*' Audio Enlightenment, p. 33
- 17 Ibid, pp. 172-173
- 18 Putney A (2017) 'Atlantean Names' *Human Resonance*, online
· http://www.human-resonance.org/3_Atlantean_Names.pdf
- 19 Putney A (2013) '*The Schildmann Decipherment*' *Human Resonance*, online
· http://www.human-resonance.org/Schildmann_Decipherment.pdf
- 20 -- (2023) 'Units of Ionizing Radiation' *Arpansa*, online
· <https://www.arpansa.gov.au/understanding-radiation/what-is-radiation/radiation/measurement>

- ²¹ Feinendegen LE, Pollycove M, Sondhaus CA (2004) 'Responses to Low Doses of ionizing Radiation in Biological Systems' *Nonlinearity in Bio, Tox & Med* 2, pp. 153-156, online
· <https://www.ncbi.nlm.nih.gov/pmc/articles/PMC2657485/pdf/nbtm-2-3-0143.pdf>
- ²² Putney A (2021) 'The Chalice of Life' *Human Resonance*, online
· http://www.human-resonance.org/Chalice_of_Life.pdf
- ²³ -- (2015) 'Homology-Dependent Double Strand Break Repair' *Youtube*, online · <https://youtu.be/86JCMM5kb2A>
- ²⁴ Mladenova V, Mladenov E, Stuschke M, Iliakis G (2022) 'DNA Damage Clustering After Ionizing Radiation and Consequences in the Processing of Chromatin Breaks' *Molecules* 27(5), online
· <https://www.mdpi.com/1420-3049/27/5/1540>
- ²⁵ Putney A (2022) 'Rasayana Elixirs of Agharta' *Human Resonance*, online
· http://www.human-resonance.org/Rasayana_Elixirs_of_Agharta.pdf
- ²⁶ Savona D (2018) 'America 's Oldest Man, Age 112, Smokes A Dozen Cigars Per Day' *Cigar Aficionado* , online
· <https://www.cigaraficionado.com/article/america-s-oldest-man-age-112-smokes-a-dozen-cigars-a-day>
- ²⁷ Putney A (2017) 'Cannabis Smoke & Psychoacoustics' *Human Resonance*, online
· http://www.human-resonance.org/Cannabis_Smoke.pdf
- ²⁸ Putney A (2017) 'The Dzopa Discs & Mc²⁹⁶' *Human Resonance*, online
· http://www.human-resonance.org/Dzopa_Discs_&_Mc296.pdf
- ²⁹ Op cit, Putney 'Rasayana Elixirs of Agharta' p. 67
- ³⁰ -- (2023) 'Oklahoma Mystery Stones' *TreasureNet*, online
· <https://www.treasurenet.com/threads/oklahoma-mystery-stones.49434/>
- ³¹ Putney A (2018) 'One' *Human Resonance*, pp. 104-113, online · <http://www.human-resonance.org/One.pdf>
- ³² Bigu J, Hussein MI, Hussein AZ (2000) 'Radiation Measurements in Egyptian Pyramids and Tombs - Occupational Exposure of Workers and the Public' *J Env Rad* 47(3), pp. 245-252